Acquisition of *in vitro* and *in vivo* functionality of Nurr1-induced dopamine neurons

Chang-Hwan Park,[*,§] Jin Sun Kang,[*,§] Yeon Ho Shin,[*,§] Mi-Yoon Chang,[†,§] Seungsoo Chung,[‖] Hyun-Chul Koh,[‡,§] Mei Hong Zhu,[¶] Seog Bae Oh,[¶] Yong-Sung Lee,[†,§] Georgia Panagiotakos,[**] Vivian Tabar,[**] Lorenz Studer,[**] and Sang-Hun Lee[†,§,1]

Departments of *Microbiology, [†]Biochemistry and Molecular Biology, and [‡]Pharmacology, College of Medicine, and [§]Institute of Mental Health, Hanyang University, Seoul, Korea; [‖]Department of Physiology, College of Medicine, Yonsei University, Seoul, Korea; [¶]Department of Physiology, College of Dentistry and Dental Research Institute, Seoul National University, Seoul, Korea; and **Laboratory of Stem Cell and Tumor Biology, Neurosurgery and Developmental Biology, Sloan Kettering Cancer Institute, New York, New York, USA

ABSTRACT **Neural precursor cells provide an expandable source of neurons and glia for basic and translational applications. However, little progress has been made in directing naive neural precursors toward specific neuronal fates such as midbrain dopamine (DA) neurons. We have recently demonstrated that transgenic expression of the nuclear orphan receptor Nurr1 is sufficient to drive dopaminergic differentiation of forebrain embryonic rat neural precursors *in vitro*. However, Nurr1-induced DA neurons exhibit immature neuronal morphologies and functional properties and are unable to induce behavioral recovery in rodent models of Parkinson's disease (PD). Here, we report on the identification of key genetic factors that drive morphological and functional differentiation of Nurr1-derived DA neurons. We show that coexpression of Nurr1, Bcl-XL, and Sonic hedgehog (SHH) or Nurr1 and the proneural bHLH factor Mash1 is sufficient to drive naive rat forebrain precursors into neurons exhibiting the biochemical, electrophysiological, and functional properties of DA neuron *in vitro*. On transplantation into the striatum of Parkinsonian rats, precursor cells engineered with Nurr1/SHH/Bcl-XL or Nurr1/Mash1 survived *in vivo* and differentiated into mature DA neurons that can reverse the behavioral deficits in the grafted animals.—Park, C.-H., Kang, J. S., Shin, Y. H., Chang, M.-Y., Chung, S., Koh, H.-C., Zhu, M. H., Oh, S. B., Lee, Y.-S., Panagiotakos, G., Tabar, V., Studer, L., and Lee, S.-H. Acquisition of *in vitro* and *in vivo* functionality of Nurr1-induced dopamine neurons. *FASEB J.* 20, E1910–E1923 (2006)**

Key Words: Parkinson's disease · neural precursor cell · transplantation · dopaminergic differentiation · dopamine neuron · Bcl-XL · Sonic hedgehog · Mash1

Neural precursors isolated from the embryonic central nervous system (CNS) can be proliferated *in vitro* and differentiated into various neuronal and glial subtypes *in vitro* and *in vivo* [for review, see (1)]. Studies on CNS precursor cells provide a valuable tool for probing brain development and for developing a renewable source of specialized neurons for cell replacement strategies. Parkinson's disease (PD) is a neurodegenerative disorder characterized by the progressive loss of midbrain dopamine (DA) neurons. Clinical experience with cell replacement in PD using fetal tissue grafts has spanned more than 10 years (2). However, efficient DA neuron differentiation from neural precursors *in vitro* has been reported only from those of embryonic ventral midbrain origin (3). Furthermore, the potential for dopaminergic differentiation of midbrain neural precursors is progressively lost during *in vitro* cell expansion (4). Given the limited success in driving dopaminergic differentiation in naive neural precursors using extrinsic cues, studies have been initiated to induce dopaminergic fate via forced expression of key transcription factors.

Mice lacking the steroid receptor-type transcription factor Nurr1 exhibit a specific loss of midbrain DA neurons (5–7). We recently demonstrated that ectopic expression of Nurr1 is sufficient to induce a dopaminergic phenotype in neural precursor cells from regions that do not typically yield DA progeny, such as rat embryonic and fetal cortical precursors (8). This study further showed that Nurr1-mediated induction of DA phenotype can be observed in neural precursors of multiple CNS regions and developmental stages (8). However, Nurr1-induced DA cells were morphologically and functionally immature, and no behavioral improvement was observed on transplantation into 6-hydroxydopamine (6-OHDA) lesioned rats. These findings suggest that Nurr1 is not sufficient to induce fully mature DA neuron progeny from neural precursors and that additional factors are required to yield DA neurons capable of restoring *in vivo* function.

[1] Correspondence: Department of Biochemistry and Molecular Biology, College of Medicine, Hanyang University, #17 Haengdang-dong, Sungdong-gu, Seoul 133–791, Korea. E-mail: leesh@hanyang.ac.kr

doi: 10.1096/fj.06-6159fje

0892-6638/06/0020-1910 © FASEB

Here we present data on the identification of cofactors sufficient to promote the differentiation and maturation of Nurr1-induced DA neurons. Combinatorial genetic modification of sonic hedgehog (SHH) and Bcl-XL or Mash1 in neural precursors allows the generation of Nurr1-induced DA neurons with improved functionality capable of reversing dopaminergic deficits in a rodent model of PD.

MATERIALS AND METHODS

Primary cultures for rat embryonic cortical precursor cells

Cultures for neural precursor cells were performed as described previously (8). Briefly, cortices were dissected from E14 rat embryos (Sprague Dawley, KOATECK, Seoul, Korea) and triturated in Ca^{2+}/Mg^{2+}-free (CMF)-HBSS (Invitrogen, Carlsbad, CA, USA). Cells were plated at 20,000 cells/cm^2 on coverslips (for unpassaged (P0) cultures, 12 mm diameter; Carolina Biological Supply Company, Burlington, NC, USA) or 10 cm tissue culture dishes (for cultures to be passaged (P1), Corning, Corning, NY, USA) precoated with polyornithine/fibronectin). Neural precursor cells were proliferated in N2 medium (9) supplemented with 20 ng/mL basic fibroblast growth factor (bFGF; R&D Systems, Minneapolis, MN, USA). Precursors reaching 60–80% cell confluency (typically requiring 3–4 d of *in vitro* bFGF-expansion) were incubated for 1 h in CMF-HBSS followed by mechanical trituration and replating onto precoated coverslips in N2+bFGF (P1 dissociate). For some experiments, CMF-HBSS incubated precursors were dislodged with a cell lifter (Corning) and directly replated onto polyornithine/fibronectin-coated coverslips without further trituration (P1 cluster). Retroviral transductions were carried out in P1 or P0 cells at 50–60% confluency (typically 1–2 d after cell plating; see below). Cell differentiation was induced by bFGF withdrawal in N2 medium supplemented with 200 μM ascorbic acid (AA, Sigma, St. Louis, MO, USA). Cultures were maintained at 37°C in 5% CO_2, media changes were carried out every other day and bFGF was supplemented daily. In some experiments, Sonic hedgehog (SHH, R&D Systems) or cyclopamine (Toronto Research Chemicals, North York, Canada,) were added to cultures.

Retroviral production and infection

The construction of the expression vectors used in this study was based on the retroviral vectors pIRES-LacZ or pIRES-GFP described previously (10). The retroviral vectors pNurr1-IRES-LacZ and pNurr1-IRES-GFP (N) expressing Nurr1 were constructed by inserting a Nurr1 cDNA fragment amplified by polymerase chain reaction (PCR) into the site upstream to the IRES element of pIRES-LacZ and pIRES-GFP, respectively. The Nurr1 sequence in pNurr1-IRES-LacZ vector was substituted by N-SHH (kindly provided by Haeyoung Suh-Kim, Ajou University, Suwon, Korea), Smo-M2 (kindly provided by Arnon Rosenthal, Genentech, Inc., San Francisco, CA, USA), Bcl-XL, Mash1, Ngn1, or Ngn2 to generate the respective expression vectors. The bicistronic [pNurr1-IRES-SHH (NH), pNurr1-IRES-Bcl-XL (NB), and pNurr1-IRES-Mash1 (NM)] or tricistronic vectors [pNurr1-IRES-SHH-IRES-Bcl-XL (NHB)] were constructed by replacing LacZ of pNurr1-IRES-LacZ with the respective cDNA fragments. The retroviral vectors were transfected into 293 gpg packaging cells (Lipofectamine®, Invitrogen) and supernatant containing viral particles (VSV-G pseudotyped recombinant retrovirus) was harvested 72 h after incubation. Viral titers were adjusted to 5×10^6 particles/ml. Neural precursors were exposed to viral supernatant for 2 h in the presence of polybrene (1 μg/ml), cultured overnight in N2+bFGF, and differentiated the following day by withdrawal of bFGF. Coexpression studies were carried out by infecting cells with the bi-/tricistronic vectors or mixtures of the individual viral constructs (1:1, v:v).

Cell viability assays

The total number of viable cells was monitored over the whole experimental period under phase-contrast microscopy. Cells with fragmented and condensed apoptotic nuclei were visualized by 4′,6′-diam idino-2-phenylidole (DAPI) staining. Cell viability was further determined by the lactate dehydrogenase (LDH) assay (Promega, Madison, WI, USA), terminal deoxynucleotidyl transferase (TdT)-mediated dUTP nick end labeling (TUNEL) assay (Roche, Mannheim, Germany), and immunocytochemistry against cleaved caspase 3. LDH activities in the medium were measured by Cytotox 96 nonradioactive kit (Promega) following the recommendations of the manufacturer. Results were expressed as percentages of maximum LDH release obtained following cell lysis by 1% Triton X-100. Culture medium was used as negative control.

Reverse transcriptase-polymerase chain reaction (RT-PCR) and Immunoblot analyses

Total RNA preparation, cDNA synthesis and RT-PCR reactions were performed as described previously (8). Primer sequences (forward and backward), annealing temperatures, PCR cycle numbers, and product sizes (base pairs) were as follows: Otx1 (5′-GCTGTTCGCAAAGACTCGC-TAC-3′, 5′-ATGGCTCTGGCACTGATACGGATG-3′, 62°C, 30 cycles, 425 bp); Emx2 (5′-TTCGAACCGCCT-TCTCGCCG -3′, 5′-TGAGCCTTCTTCCTCTAG -3′, 59°C, 35 cycles, 188 bp); Pax6 (5′-CCAAAGTGGTGGACAAGAT-TGCC-3′, 5′-TAACTCCGCCCATTCACTGACG-3′, 58°C, 35 cycles, 419 bp); SHH (5′-GGAAGATCACAAACTCCGAAC-3′, 5′-GGATGCGAGCTTTGGATTCATAG-3′, 58°C, 32 cycles, 354 bp); Smo (5′-TGCTGTGTGCTGTCTACATGCC-3′, 5′-TCTTGGGGTTGTCTGTCCTCAC-3′, 58°C, 32 cycles, 240 bp); Ptc (5′-GGCAAGTTTTTGGTTGTGGGTC-3′, 5′-CCATGTAACCTGTCTCCGTGATAAG-3′, 58°C, 35 cycles, 355 bp); Bcl-XL (5′-CAAGCTTTCCCAGAAAGGAT-3′, 5′-TGAAGAGTGAGCCCAGCAGA-3′, 58°C, 33 cycles, 702 bp); Synapsin (5′- CCACCCCCACAAGGCCAGCA ACA-3′, 5′- GGTCCCCCGGCAGCAGCAATGATG-3′, 58°C, 29 cycles, 512 bp); Synaptophysin (5′-TGGTATCCTACCG-CATTC-3′, 5′-ACTCACCTCATAGCTCC-3′, 58°C, 26 cycles, 379 bp); GAP43 (5′-AGAAAGCAGCCAAGCTGAGGAGG-3′, 5′-CAGGAGAGACAGGGTTCAGGTGG-3′, 58°C, 26 cycles, 167 bp); Rho8 (5′-ACGGGAAGCAGGTAGAGTTG-3′, 5′-GATGGGCACATTTGGACAG-3′, 58°C, 21 cycles, 191 bp); Scg10 (5′-CTACCCGGAGCCTCGCAAC-3′, 5′-ACC-TGGGCCTCCTGAGACTTC-3′, 58°C, 21 cycles, 231 bp); GAPDH (5′-GGCATTGCTCTCATTGACAA-3′, 5′-AGGGC-CTCTCTCTTGCTCTC-3′, 25°C, 60 cycles, 165 bp).

Proteins were extracted from cultured cell lysates, electrophoresed, and transferred to nitrocellulose membrane as described previously (11). The blot was probed with an anti-mouse neuron-specific class III β-tubulin (TuJ1, Covance, Richmond, CA, USA, 1:1,000), tyrosine hydroxylase (TH, Sigma, 1:5,000), β-actin (Abcam, Cambridge, UK, 1:5000) antibodies, followed by anti-mouse or rabbit IgG conjugated with peroxidase (Cell Signaling Technology, Beverly, MA, USA, 1:2000). Bands were visualized with enhanced chemiluminescence (ECL) detection kit (Amersham Pharmacia, Buckinghamshire, UK).

DA level determination and DA uptake assay

HPLC analysis for DA level was performed as described previously (11) with some modification. To determine *in vitro* DA release from cultured cells, differentiated precursor cells in 24-well plates were incubated in 500 μl N2 + AA medium for 24 h or 15 min (basal release) or in the same medium supplemented with 56 mM KCl for 15 min (evoked release). The media were then collected and stabilized in 0.1 N perchloric acid (PCA) containing 0.1 mM EDTA and extracted by aluminum adsorption. To measure DA amounts in the grafts of transplanted animals, tissues from the center of grafts (~2 mm diameter in size) were homogenized in 0.2 N PCA containing 0.1 mM EDTA and then centrifuged at 5000 g for 10 min. The supernatants were filtered through centrifugal filter devices (microcon YM-10, Millipore Co., Billerica, MA, USA) at 12,000 g for 10 min, and used for DA level determination. DA was separated with a reverse phase μ-Bondapak C18 column (150×3.0 mm, Eicom, Japan) at a flow rate of 0.5 ml/min. Electroactive compounds were analyzed at +750 mV using an analytical cell and an amperometric detector (ECD-300, Eicom). DA levels were calculated using an internal standard (50 nM methyl-DOPA) and catecholamine standard mixtures including 1–50 nM DA (external standard) injected immediately before and after each experiment. DA transporter (DAT)-mediated specific DA uptakes were carried out as described recently for characterizing human ES cell-derived DA neurons (12).

Electrophysiology

Electrophysiological analyses were performed by whole-cell recording using standard whole-cell patch-clamp techniques. Nurr1-expressing cells were identified by GFP expression (Nurr1-IRES-GFP). Coexpression studies of Mash1 or SHH+Bcl-XL in Nurr1-expressing cells were performed as described above. After 10 d of *in vitro* differentiation, individual GFP+ Nurr1-expressing cells were selected for the electrophysiological analyses. The patch electrodes had resistances of 2 to 4 MΩ. The cell membrane capacitance and series resistance were compensated (typically >80%) electronically using a patch-clamp amplifier (Axopatch-200A; Axon Instruments, Foster City, CA, USA). Current protocol generation and data acquisition were performed using pClamp 8.2 software on an IBM computer equipped with an analog-to-digital converter (Digidata 1322A; Axon Instruments). All experiments were performed at room temperature (21–24°C). For recording of membrane potential in current clamp mode, the patch pipette solution contained (in mM): KCl 134, $MgCl_2$ 1.2, MgATP 1, Na_2GTP 0.1, EGTA 10, glucose (Glc) 14, and HEPES 10.5 (pH adjusted to 7.2 with KOH). The bath solution contained (in mM); NaCl 134, KCl 5, $CaCl_2$ 2.5, $MgCl_2$ 1.2, Glc 14, and HEPES 10.5 (pH adjusted to 7.4 with NaOH).

Immunostaining on cultured cells and brain slices

Cultured cells or cryosectioned brain slices were fixed in 4% paraformaldehyde/0.15% picric acid in PBS and incubated with primary antibodies overnight at 4°C. The following primary antibodies were used: anti-rabbit TH (Pel-Freez, Rogers, AR, USA, 1:250), TuJ1 (Covance, 1:2000), anti-mouse-TH (Sigma, 1:10,000), anti-GFP (Roche, 1:400) and microtubule-associated protein 2(a+b) (MAP2, Sigma, 1:500), anti-rabbit cleaved caspase 3 (Cell Signaling, 1:200). Appropriate fluorescence-tagged (Jackson Immunoresearch Laboratories, West Grove, PA, USA) secondary antibodies were used for visualization. Cells and tissue sections were mounted in VECTASHIELD® containing DAPI (Vector Laboratories, Burlingame, CA, USA) and analyzed under either an epifluorescence microscope (Nikon, Tokyo, Japan) or a Carl Zeiss LMS 510 confocal system (Carl Zeiss, Jena, Germany).

Morphometric analysis for neurite outgrowths

The neurite length of TH+ cells was measured as described previously (8). Briefly, 20–50 TH+ cells were randomly selected from at least three cultures from three independent experiments. Cells were photographed on an Axiovert Phase-Contrast Microscope equipped with an Axiocam digital camera system, and the neurite lengths from the soma to the tip of the branches were measured using Axiovision image analyzer (Carl Zeiss). The total neurite length was defined as the combined length of all neurites per cell.

Surgical procedures and behavioral testing

Animals were housed and treated following National Institutes of Health guidelines. Female, Sprague-Dawley rats (200–250 g) were lesioned by unilateral stereotactic injection of 6-OHDA (Sigma) into the substantia nigra and the median forebrain bundle as described previously (11). Four weeks after the lesioning, animals were tested for drug-induced rotational asymmetry (Amphetamine 3 mg/kg i.p., Sigma). Rotation scores were monitored for 60 min. in an automatized rotometer system (Med Associate Inc., St. Albans, VT, USA). Animals with ≥5 turns/min ipsilateral to the lesion were selected for transplantation. Forelimb akinesia was measured by "step adjustment test" (13), as described previously (11), three times prior to grafting and repeated in weekly intervals for 8 wk after cell transplantation. The number of adjusting steps of the unrestrained forelimb was counted while the animal was moved in backwards direction (90 cm in 10 s). The percentage of steps on the lesioned side *vs.* unlesioned side was quantified (average of three trials/time point).

Two days after retroviral infection, bFGF expanded precursors were mechanically dissociated, and 3 μl of the cell suspension (1.5×10^5 cells/μl in PBS) was injected (22 G needle) over a 5 min period into the ipsilateral striatum using KDS310 nano pump (KD Scientific Inc., Holliston, MA, USA). Cells were deposited at 3 sites (coordinates in AP, ML and V relative to bregma and dura (1) −0.03, −0.30, −0.58; (2) −0.03, −0.40, −0.58; (3) 0.03, −0.35, −0.58; incisor bar set at 3.5 mm). The needle was left in place for 5 min following each injection. The rats received daily injections of cyclosporin A (10 mg/kg, i.p.), starting 24 h prior to grafting and continuing for 3 wk followed by a reduced dose of 5 mg/kg for the remaining time.

Histological procedures

Animals were anesthetized (50 mg/kg penobarbital) and intracardially perfused with 4% paraformaldehyde in PBS. Brains were equilibrated in 20% sucrose in PBS and sectioned at 35 μm on a freezing microtome. Free-floating sections were subjected to TH-immunohistochemistry as described above. Estimation of TH+ cell numbers were made as described previously (11).

Cell counting and statistic analysis

Cell counting was performed by uniform random selection of 5–20 microscopic fields/well, 3–6 wells/experimental condition, and data were confirmed in more than three independent experiments. Data are expressed as mean ± SEM.

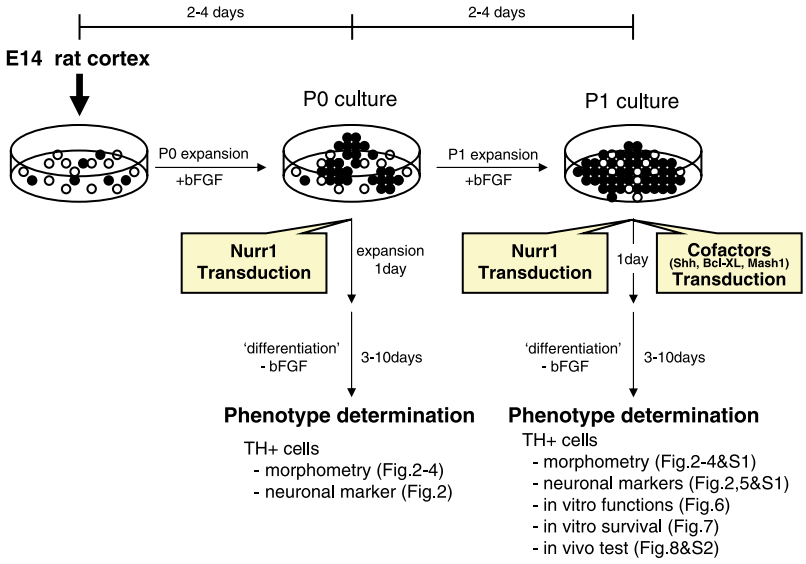

Figure 1. Schematic illustration of the experimental procedures. Neural precursor cells were isolated from rat embryonic cortices at E14 and cultured in the presence of bFGF for 2–4 d. For preparing passaged cultures, the expanded precursors were harvested, plated onto FN-coated surfaces freshly prepared, and further proliferated with bFGF for additional 2–4 d. The proliferated unpassaged (P0) and passaged (P1) precursor cells were retrovirally transduced with Nurr1 and other cofactors. One day after transduction, precursor differentiation was induced by withdrawal of bFGF. The phenotype of the differentiated cells was assessed *in vitro* and *in vivo* after 3–10 d of mitogen withdrawal.

Statistical comparisons were made by ANOVA with Tukey post hoc analysis (statistical Packages for the Social Sciences 12.0; statistical Packages for the Social Sciences (SPSS) Inc., Chicago, IL, USA) when more than two groups were involved.

RESULTS

Neuronal differentiation of Nurr1-induced DA cells from unpassaged (P0) and passaged (P1) rat embryonic neural precursor cells

While forced expression of Nurr1 induces DA neurotransmitter identity in various neural precursors (8, 14, 15), the level of neuronal differentiation is highly variable among these cells. Nurr1 expressing long-term expanded adult neural precursors do not exhibit neuronal properties (14). However, neuronal identity was reported in subpopulations of short-term expanded Nurr1-induced embryonic neural precursors (8). These findings suggest that neuronal differentiation in Nurr1-induced DA cells may depend on the duration of *in vitro* expansion or the developmental stage of the precursor cells. Our previous study on Nurr1-induced neural precursors was carried out in passaged (P1) cells on several days of *in vitro* expansion followed by mechanical trituration and replating (8). These conditions were chosen to ensure high purity of neural precursors (>95% nestin+cells, <1% of TuJ1+ neurons) in contrast to unpassaged neural precursors (P0) that contain up to 15% postmitotic neurons (16).

Here we compared the level of neuronal differentiation in Nurr1-induced DA cells at P0 and P1 (**Fig. 2**). Precursors were transduced with Nurr1-retroviruses at the last day of the precursor cell expansion (P0: *in vitro* day 3; P1: *in vitro* day 6). Cells were differentiated for an additional 3–10 d prior to analysis. We first examined Nurr1 effects on cell apoptosis and morphology. In Nurr1-transduced P0 and P1 cultures, cell apoptosis was increased as compared with LacZ-transduced control cultures. Three days after differentiation, percentages of cells with apoptotic nuclei (fragmented or condensed) were significantly increased in Nurr1-transduced cultures compared with lacZ-transduced control cultures: 16.5 ± 1.0% *vs.* 10.9 ± 0.8% in P0 cultures; 15.7 ± 0.8% *vs.* 10.6 ± 0.5% in P1 cultures (n=35–60 microscopic fields from 3–8 coverslips, P<0.001). Interestingly, neurite length was significantly decreased in cells transduced with Nurr1 (Nurr1-IRES-GFP), compared with control cultures (LacZ-IRES-GFP) (Fig. 2*A–D*). The mechanisms responsible for the increased rate of apoptosis and the decreased morphological differentiation in Nurr1-transduced cells are currently unclear.

In both P0 and P1 cultures, Nurr1 transduction efficiently induced expression of TH, a specific marker expressed in DA neurons (Fig. 2*E–H*). Morphometry of Nurr1-induced DA cells revealed a marked increase in total length of TH+ fibers in P0 cultures compared with P1 cultures (P0: 84.0±4.9 μm; P1: 14.2±5.7 μm, n=40–50, P<0.001, Fig. 2*F*, *H*). Consistent with the data on morphological differentiation, a larger proportion of TH+ cells expressed the neuronal markers TuJ1 and MAP2 in P0 cultures compared with P1 cultures. At day 3 of *in vitro* differentiation, TuJ1 was colocalized in 37.3 ± 2.4% (P0) and 8.6 ± 1.2% (P1) of TH+ cells (n=25, P<0.001, Fig. 2*I*, *J*). MAP2 expression was observed in 65.0 ± 4.7% of all TH+ cells at P0 and in 11.7 ± 1.8% of TH+ cells at P1 at day 10 of *in vitro* differentiation (n=30, P<0.001, Fig. 2*K*, *L*). These findings indicate that Nurr1-TH+ cells in P0 cultures exhibit a higher degree of neuronal differentiation in P0 cultures compared with P1 cultures.

SHH-mediated morphological differentiation of Nurr1-TH+ cells

The main differences between P0 and P1 cultures are the longer period of *in vitro* precursor cell expansion in P1 cells (6 d in P1 *vs.* 3 d in P0) and the mechanical passaging of P1 (P0 cells are not passaged). We first

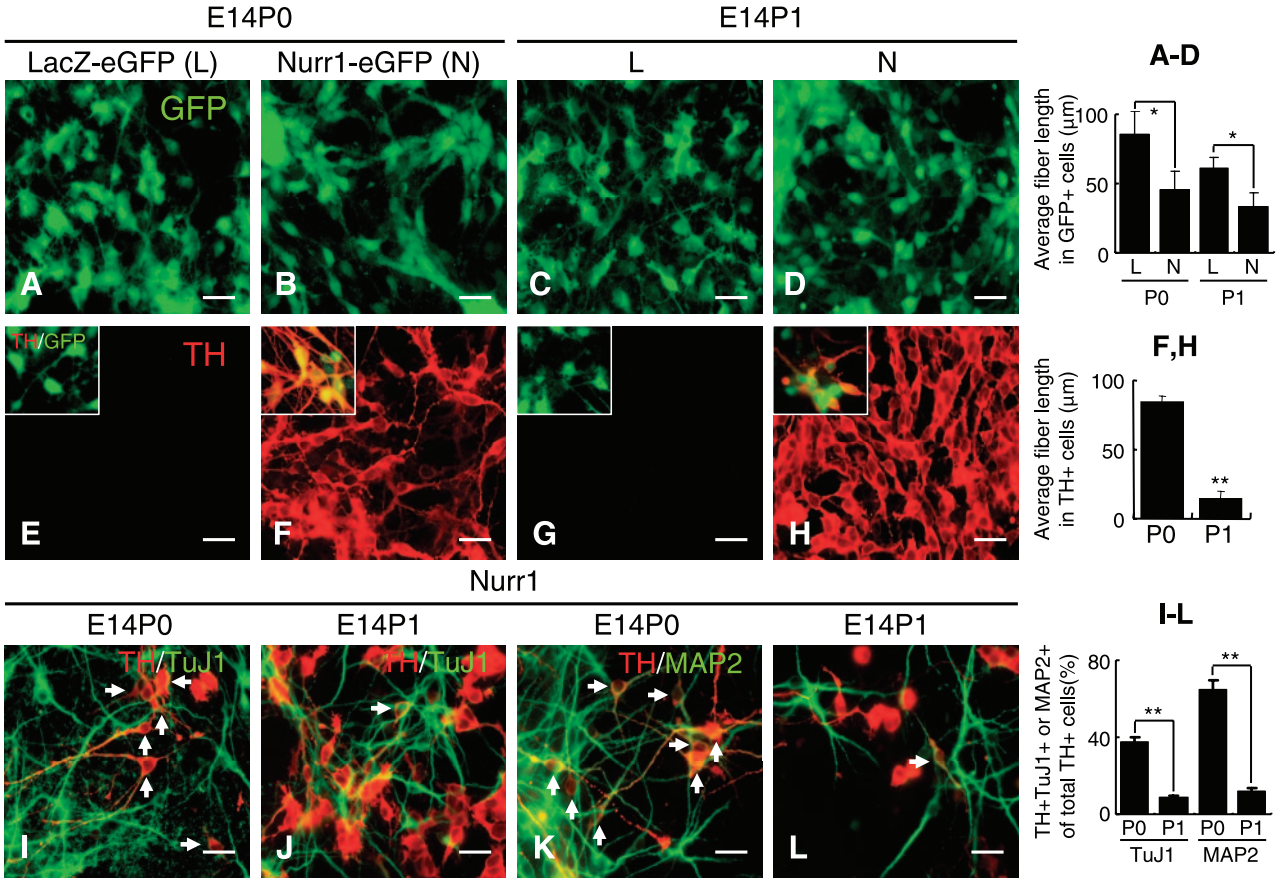

Figure 2. Neuronal differentiation of Nurr1-induced DA cells in unpassaged (P0) and passaged (P1) cultures. P0 and P1 cortical precursor cells were transduced with viruses carrying the Nurr1 transgene (Nurr1-IRES-GFP) or LacZ (LacZ-IRES-GFP; control). Transduced neural precursors were differentiated for 3 (*A–J*) or 10 d (K, L) prior to analysis. *A–D)* Effects of Nurr1 transduction on cell morphology of cultured precursor cells. At day 3 of *in vitro* differentiation, total length of GFP+ processes was assessed in Nurr1-transduced and lacZ control cultures. Images on left show representative GFP-immunocytochemistry, right graph provides quantification (mean±SEM of total GFP+ fiber length per cell, n=30–40 GFP+ cells for each value). *Significantly different from LacZ-transduced control values at $P < 0.01$. *E–H)* Difference in morphological differentiation of Nurr1-DA cells in P0 and P1 cultures. Transgenic expression of Nurr1 in P0 and P1 precursors efficiently induced TH expression, a marker of DA neurons. The length of TH+ fibers was quantified at day 3 of differentiation. Insets of (*E–H*) are images of TH+/GFP+ cells obtained by double immunohistochemistry. The right panel depicts quantification of average TH fiber length per cell obtained from 40 and 50 TH+ cells in P0 and P1 cultures, respectively. *I–L)* Neuronal maker expression in Nurr1-induced TH+ cells. Nurr1-transduced P0 and P1 cells were subjected to immunocytochemistry for TH/TuJ1 (*I, J*) at day 3 or TH/MAP2 (K,L) at day 10 of *in vitro* differentiation. The right graph depicts the proportions of TH+ cells expressing TuJ1 or MAP2 out of the total number of TH+ cells. Arrows in (*I–L*) indicate TH+ cells expression TuJ1 (*I, J*) or MAP2 (*K, L*). n = 20–25 microscopic fields from three coverslips. Scale bar, 10 μm. **Statistically significant at $P < 0.001$.

examined whether the mechanical passaging procedure may be responsible for the decreased level of neuronal differentiation in Nurr1-induced DA cells in P1 *vs.* P0 cultures. Our routine passaging procedure (see Materials and Methods) is based on CMF-HBSS incubation followed by mechanical trituration of the cell clusters to single cell suspensions (9). To test the effect of cell-to-cell interactions, we passaged parallel cultures by replating cell clusters without trituration (P1 clusters). Interestingly, under these conditions the morphological differentiation of the Nurr1-TH cells was not significantly altered compared with P0 cultures, whereas that of P1 cultures with single-cell suspension (P1 dissociates) were much poorer than P0 [**Fig. 3*A–C***; P0 cultures (P0): 67.5 ± 4.2 μm; P1 clusters (P1C): 43.0 ± 11.7 μm; P1 dissociates (P1D): 9.3 ± 0.7 μm, n = 25–30]. These data demonstrate that disruption of cell-to-cell contacts during passaging negatively affects neuronal maturation of Nurr1-induced DA cells. Reduced length of TH+ fibers in P1 culture is not likely to be due to the loss of cellular processes during mechanical trituration. It is because we applied very similar levels of mechanical trituration to the dissected cortical tissue at the time of preparation compared to the cells passaged for P1 culture. Consistently, we could not observe major differences in cell morphology 6–24 h after cell plating comparing P0 and P1 cultures (data not shown).

We wanted to gain a molecular understanding of the differences observed between triturated and nontriturated P1 Nurr1-induced DA cells. Gene expression profiles were established from neural precursors in P0,

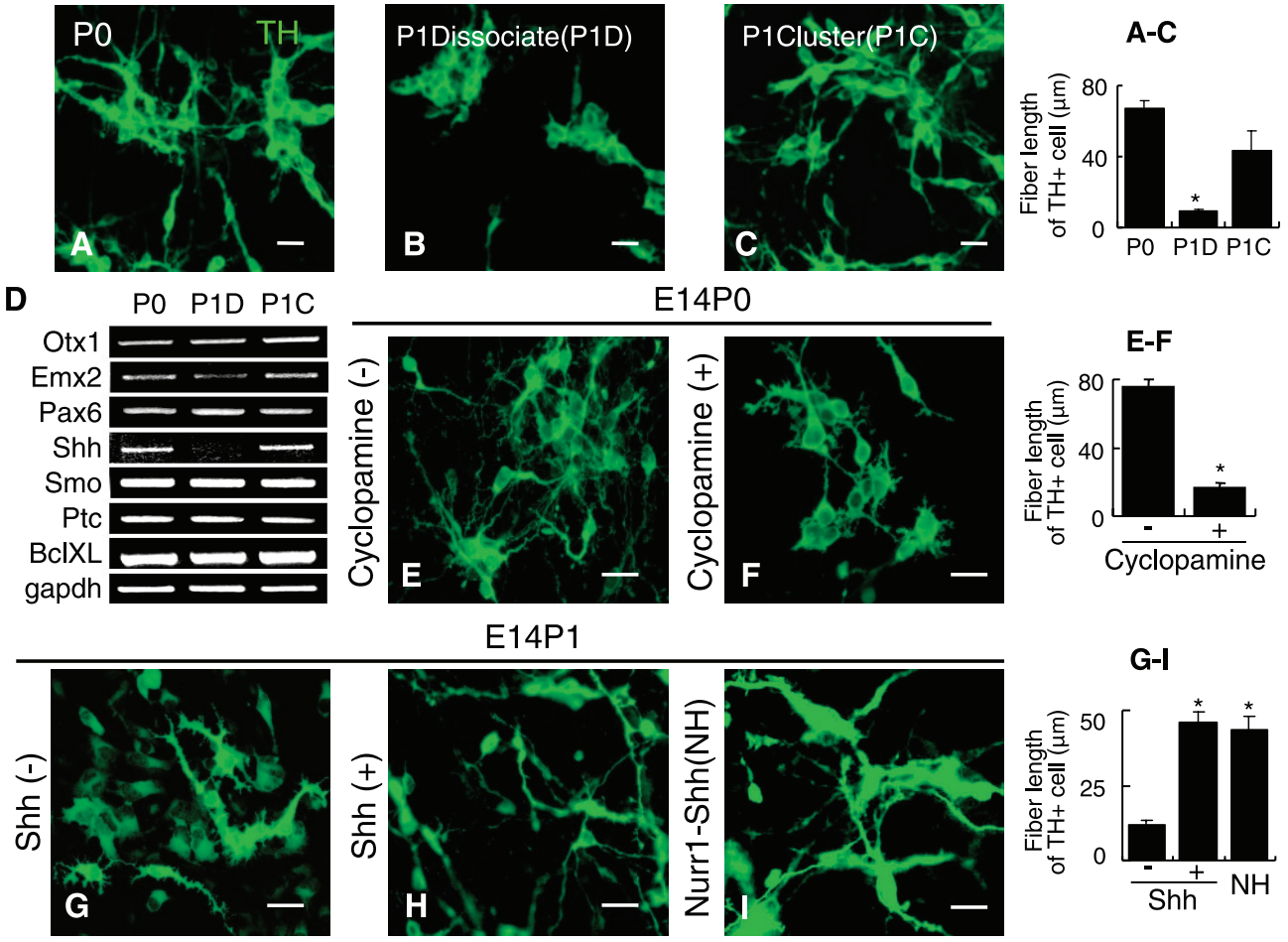

Figure 3. Enhanced morphological differentiation of Nurr1-DA cells by SHH. *A–C)* Nurr1-induced TH+ cells derived from E14 cortical precursors at P0 (*A*) or from precursors passaged by mechanical trituration to single cell density (P1Dissociate, P1D; *B*) or passaged by maintaining intact cell-cell contacts (P1Cluster, P1C; *C*). *D)* Semiquantitative RT-PCR analysis of P0, P1D, and P1C cultures for genes related to forebrain development and SHH signaling. Note that SHH expression was lost after disruption of cell-cell contacts in P1D culture under conditions that led to poor morphological differentiation of Nurr1-TH cells. *E–I)* Effects of SHH signaling on the differentiation of Nurr1-TH cells. Reduced neurite length of Nurr1-TH cells on cyclopamine treatment (1 μg/ml) in P0 cultures (*E, F*). Increased morphological differentiation of Nurr1-TH cells at P1 was observed on SHH treatment (500 ng/ml) (*H*) or after transgenic expression of SHH in combination with Nurr1 (Nurr1-IRES-SHH) (*I*) *G–I*). Scale bar, 10 μm. Graphs in right panel present the mean ± SEM of total fiber length in a TH+ cells. Individual values were obtained by the morphometric analysis of 20–45 randomly selected TH+ cells. *Significantly different from P0 (*A–C*), untreated (*E, F* and *G, H*), and Nurr1-transduced (*G, I*) at $P < 0.001$.

P1 dissociate, and P1 cluster cultures. Among the candidate markers tested, SHH expression was completely lost in P1 dissociates, whereas it was maintained in P1 cluster cultures (Fig. 3*D*). SHH is well known for its role during early CNS patterning and the derivation of DA neurons (17, 18). However, SHH is also a powerful chemoattractant that promotes axonal growth from neighboring neurons (19, 43). We found that exposure of P1-dissociated cultures to SHH (500 ng/ml) increased TH fiber length in Nurr1-induced DA cells (SHH treated: 46.0±3.6 μm *vs.* untreated control: 11.8±1.3 μm, $n=45$, $P<0.001$; Fig. 3*G, H*). Forced expression of Smo-M2, the constitutively active form of the SHH receptor smoothened (20) or expression of the 22 kDa SHH N-terminal domain yielded comparable results (Nurr1-IRES-SHH vector, NH, 43.3±4.8 μm, $n=20$; Fig. 3*I*, and data not shown). Furthermore, neurite outgrowth of Nurr1-DA cells in P0 cultures was strikingly reduced on treatment with the well-characterized SHH inhibitor cyclopamine (1 μg/ml, Ref. 21) *vs.* control (cyclopamine: 6.5±3.0 μm; control: 76.0±3.6 μm, $n=30$, $P<0.001$; Fig. 3*E, F*). Treatment of P0 cultures with SHH or treatment of P1 cultures with cyclopamine did not induce significant changes in TH+ fiber lengths compared with untreated control cultures (data not shown). These findings suggest that loss of endogenous SHH during passaging negatively affects the differentiation of Nurr1-induced DA cells.

The role of Bcl-XL on the enhanced differentiation of Nurr1-DA cells in neural precursors derived from later developmental stages

We next tested whether the period of *in vitro* expansion affects the morphological differences observed between P0 and P1 Nurr1-TH cells. An important variable

that influences differentiation of neural precursors is cell density, with higher cell densities promoting differentiation through soluble factors secreted from the precursors (22). We minimized density-dependent effects by plating cells at low density (4000 cells/10 cm plate, ~80 cells/cm^2), followed by transduction with Nurr1 retrovirus at days 2 and 5 of proliferation (passage was not included in either of the cultures). Analysis was performed on an additional 5 d of differentiation in both day 2 and day 5 transduced cultures. Under these conditions fewer than 20 colonies of cells (average size, >1 mm) were observed per 10 cm dish. Although the colonies grew in size from day 2–5 of expansion (2-fold increase in diameter), overall cell density in the plate remained very low, making interference with paracrine factors unlikely. Interestingly, in contrast to the P0 and P1 culture data, neurite outgrowth was increased in cultures that underwent longer expansion periods (day 5 transduced cells: 6.6±1.0 μm; *vs.* day 2 transduced cells: 0.6±0.1 μm, n=20, P<0.001, **Fig. 4*A–D***).

Previous work has demonstrated distinct precursor cell properties depending on developmental stage and extent of *in vitro* proliferation (4, 16, 23). We observed that early embryonic neural precursors expanded *in vitro* start adopting properties of precursors derived from later developmental stages (16). Thus, our results on increased morphological maturation in precursors expanded for extended *in vitro* periods could reflect changes in precursor cell stage. Therefore, we next tested whether Nurr1 transduction of rat cortical precursors isolated from various developmental stages (E12-E18) yields similar differences. Consistent with our hypothesis, precursors derived from later developmental stages exhibited a higher degree of cell differentiation compared with those from earlier developmental stages (Fig. 4*E–H*; E18 P0 cultures: 101.7±5.2 μm; E16 P0: 98.2±3.0 μm; E14 P0: 74.7±8.4 μm; E12 P0: 63.5±5.1 μm, n=35–40, P<0.001). These data demonstrate that neural precursor stage affects the degree of neuronal differentiation in Nurr1-induced DA cells.

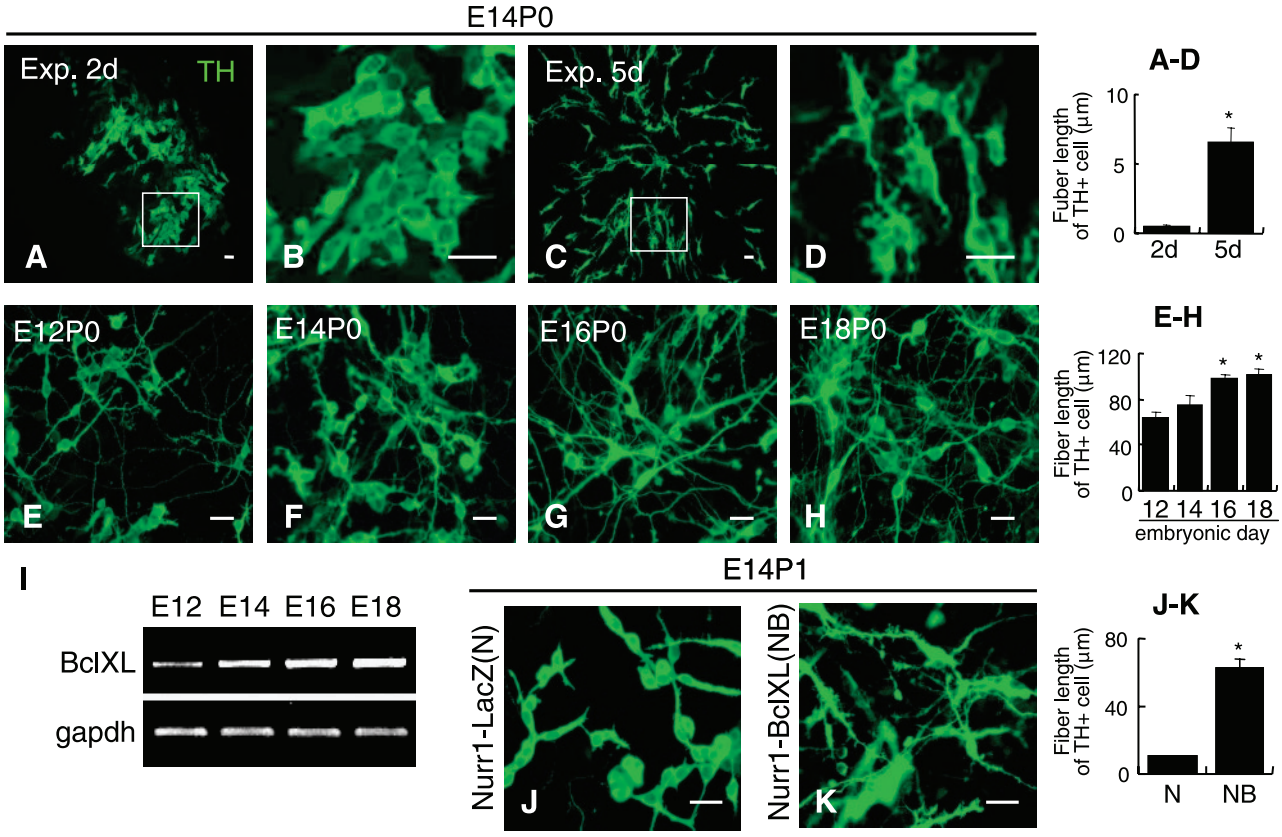

Figure 4. The role of Bcl-XL in the enhanced morphological differentiation of Nurr1-DA cells derived from precursors at later developmental stages. *A–D*) TH+ cells derived from short- (2 d; *A*, *B*) and longer-term (5 d; *C*, *D*) expanded neural precursors transduced with Nurr1. Precursor cells from E14 cortices were plated at a low cell density (4000 cells/10 cm plate) followed by transduction with Nurr1 retrovirus at days 2 and 5 of proliferation (passage was not included in either of the cultures). Morphometric analysis of TH cells was performed after an additional 5 d of differentiation. The boxed areas of (*A*) and (*C*) are magnified in (*B*) and (*D*), respectively. *E–H)* Nurr1-TH cells in P0 cultures from cortical precursors isolated from various embryonic days (E12–E18). *I)* Bcl-XL mRNA expression in cultured cortical precursors isolated at E12–E18 and cultured for 3 d in bFGF (P0). *J, K)* Enhanced neurite outgrowth in Nurr1-TH cells by coexpression of Bcl-XL. P1 precursor cells were transduced with the viruses carrying Nurr1-IRES-LacZ (control; *J*) or Nurr1-IRES-Bcl-XL (NB, *K*), and TH+ fiber length was determined at day 5 of differentiation. Scale bar, 10 μm. The right graphs represent means ± SEM of total TH+ neurite length (n=20–25 TH+ cells randomly chosen from three coverslips of each group). *Significantly different from 2 d (*A–D*), E12 (*E–H*), and N-transduced (*J–K*) at $P < 0.001$.

The antiapoptotic proteins Bcl-2 and Bcl-XL are candidate factors for enhancing DA neuron differentiation (11, 24, 25). Interestingly, increased Bcl-XL expression (Fig. 4*I*) was observed in precursors isolated from later embryonic stages, those associated with increased morphological maturation. We next tested whether forced expression of Bcl-XL enhances neuronal differentiation in Nurr1-DA cells (Nurr1-IRES-Bcl-XL vector, NB). Cells transduced with NB exhibited a marked increase in neurite length compared with Nurr1-IRES-LacZ transduced cells (N) (NB: 62.0±5.2 μm *vs.* N: 10.3±0.6 μm, $n=20–25$, $P<0.001$; Fig. 4 *J, K*).

Divergent action of bHLH factors on Nurr1-induced DA neuron differentiation

Neuronal bHLH transcriptional factors play an essential role during neuronal specification of precursor cells and during the morphological and functional maturation of postmitotic neurons [for review, see (26–29)]. Two classes of neuronal bHLH genes have been identified in drosophila, the achaete-scute and atonal family [for review, see (30, 31)], and the orthologues of these bHLH genes are expressed during mammalian brain development. Results in Nurr1-induced DA cells suggest a disconnection between acquisition of DA neurotransmitter phenotype and neuronal differentiation. We therefore tested whether the well-known neurogenic effects of bHLH proteins could overcome the limited neuronal commitment and maturation of Nurr1-induced DA cells. While all bHLH proteins showed similar effects on overall neuronal differentiation as assessed by TuJ1 (Supplemental Fig. S1*A–D, F*), a striking difference was found between achaete-scute and atonal homologues on the differentiation of Nurr1-induced DA cells. Forced expression of the achaete-scute homologue Mash1 [Nurr1-IRES-Mash1 retrovirus (NM)] caused a dramatic increase in morphological differentiation of the Nurr1-DA cells [NM: 147.4±50.9 μm *vs.* N: 9.0±1.8 μm; Supplemental Fig. S1*G–H* and (10)] without affecting TH+ cell yield (Supplemental Fig. S1*F*). Coexpression of Nurr1 and Ngn1 or Ngn2, homologues of the atonal family, caused a near complete loss of TH+ cells [Supplemental Fig. S1*A–D* and *F* (10)]; % TH+ cells out of total cells were Nurr1+LacZ (N): 41.1 ± 2.0% *vs.* Nurr1+Ngn1: 1.1 ± 0.6%, and Nurr1+Ngn2: 2.8 ± 0.9%. These findings demonstrate a powerful effect of bHLH proteins on neuronal specification and maturation but divergent effects of Mash1 *vs.* Ngn1 and Ngn2 on the DA neuron specification of Nurr1-induced neural precursors.

Bcl-XL/ SHH and Mash1 independently regulate the differentiation of Nurr1-DA cells

Additional studies showed that SHH and Bcl-XL have additive effects on neurite growth in Nurr1-DA cells [Nurr1-IRES-SHH-IRES-Bcl-XL (NHB): 82.5±1.5 μm, NH: 38.0±5.8 μm, NB: 62.2±6.1 μm, $n=25–40$]. However, we did not observe additional benefit when expressing Mash1 with either Bcl-XL or SHH, or when expressing Mash1 with both Bcl-XL+SHH in Nurr1-induced DA cells (data not shown). These findings suggest that the two novel strategies presented here (expression of Bcl-XL and SHH or expression of Mash1) may act on a common final pathway that modulates neuronal and dopaminergic differentiation in Nurr1-induced DA cells. We have tested a large number of other candidate genes that proved ineffective in our system, including among others glial-derived neurotrophic factor (GDNF), Wnt-5a, Pax2, DAT, and tissue inhibitor of metalloproteinase (TIMP) (data not shown). While it is possible that future additional cofactors may provide further benefit, the effects of Bcl-XL/SHH and Mash1 are rather specific. We therefore decided to perform subsequent *in vitro* and *in vivo* functional studies of Nurr1-DA cells in NHB-, NM-, and N-transduced cultures.

Biochemical and physiological properties of Nurr1-induced DA cells

We next tested whether enhanced morphometric maturation is correlated with the expression of mature neuronal marker MAP2. Quantification of the percentage of Nurr1-induced DA cells expressing MAP2 confirmed our morphometric data on cell differentiation (**Fig. 5*A–D***). TH+/MAP2+ cells out of total TH+ cells were 67.5 ± 4.1% (NHB), 71.0 ± 2.4% (NM), and 11.8 ± 2.1% (N).

The effects of NHB and NM on neurite growth and maturation were correlated with increased expression of transcripts associated with growth cone development (GAP43), neurite outgrowths (Rho8 and Scg10), and synapse formation (synapsin and synaptophysin) (Fig. 5*E*).

Presynaptic DA neuron function of NHB-, NM-, or N-transduced cells was assessed by measuring DA release *in vitro*. HPLC analysis revealed no detectable levels of DA at basal levels (15 min exposure to medium), but rather robust DA release on depolarization of the cells (15 min in medium containing 56 mM KCl). While all conditions exhibited KCl-induced DA release, significant quantitative differences were found among the groups (**Fig. 6*A***). DA levels were NHB: 2558.2 ± 152.4 pg/ml, NM: 3049.9 ± 377.6 pg/ml, and N: 561.2 ± 50.2 pg/ml. Functional differences in DA metabolism were further illustrated by measuring DAT-mediated high-affinity reuptake of DA. While reuptake in Nurr1 cultures was at the limit of detection (N: 0.23±0.01 fmol/min/well), NHB- and NM-transduced cells exhibited robust DA uptake (NHB: 4.59 ± 0.50 fmol/min/well, and NM: 2.90 ± 0.61 fmol/min/well; Fig. 6*B*).

Electrophysiological analysis of Nurr1-induced DA cells (NHB group) demonstrated well-developed sodium and potassium channels in cells with differentiated neuronal morphologies (data not shown) and the generation of action potentials by prolonged depolar-

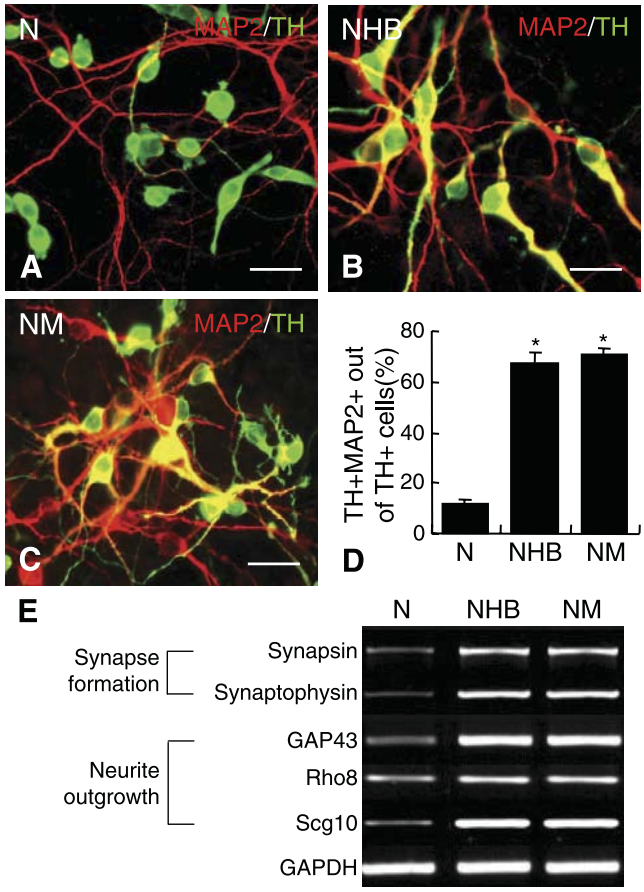

Figure 5. *A–D)* Expression of MAP2 in Nurr1-induced TH cells. TH/MAP2 immunocytochemistry was carried out at day 10 of *in vitro* differentiation in the cultures transduced with N, NM, and NHB. Graph (*D*) represents the percentages TH+ cells coexpressing MAP2 out of total TH+ cells. Each value was obtained from 25–30 microscopic fields in three coverslips. *Significantly different from the controls with the *P* value of <0.001. Scale bar, 10 μm. *E)* Semiquantitative RT-PCR analyses for markers of neurite outgrowth and synapse formation.

izing current injections (Fig. 6*C*), a hallmark feature of differentiated neurons. In addition, as the intensity of the hyperpolarizing current injections was increased, there was a time-dependent reduction in the membrane deflection (Fig. 6*D*), indicating an anomalous rectification characteristic for mesolimbic (32) and nigrostriatal (33) DA neurons. These cells also showed hyperpolarizing inward current, which can evoke anomalous rectification in current-clamp mode (Fig. 6*E*). Similar electrophysiological patterns could also be observed in the cells infected with NM (Fig. 6*F–H*).

Enhanced *in vitro* survival of Nurr1-induced DA cells by Bcl-XL/SHH and Mash1

The survival rate of transplanted DA neurons is critical for preclinical studies in animal models of PD. We therefore determined the effects of our transduction strategies on the viability of precursor progeny. Bcl-XL is one of best characterized antiapoptotic proteins, and SHH-mediated effects on the survival of neural precursors (34) and postmitotic neurons including midbrain DA neurons (35) has been demonstrated previously. Consistently, percentages of cells with apoptotic nuclei was decreased in cultures transduced with Bcl-XL (4.2±0.2%) or SHH (7.5±0.6%), compared with LacZ-transduced control cultures (11.3±0.6%, n=40 microscopic fields from four coverslips, significantly different from LacZ-transduced control values at P<0.001). We next examined more closely the effects of Bcl-XL, SHH, and Mash1 on the survival of Nurr1-transduced precursor cells. NHB-transduced cells showed a marked increase in cell viability compared with Nurr1-only (N) cultures. Data are provided on the total number of cells, the total number of TH+ cells, LDH release, percentage of cells with apoptotic nuclei, percentage of TUNEL+ cells, and percentage of cells positive for activated caspase 3 (**Fig. 7**). Cell survival in cultures transduced with NHB was significantly greater than in cultures transduced with NH or NB, suggesting additive roles for SHH and Bcl-XL on cell survival. Interestingly, coexpression of Mash1 in Nurr1-transduced cells (NM) also resulted in enhanced survival for all indices tested above.

In vivo transplantation studies

The final set of experiments was directed at addressing the capacity of Nurr1-induced DA cells for *in vivo* survival, integration, and function in Parkinsonian rats. Precursors transduced with N, NM, and NHB were transplanted into the adult striatum of rats with a unilateral 6-OHDA lesion. Histological analysis was performed at 4 and 8 wk after transplantation. Both NHB- and NM-transduced precursors showed a dramatic increase in the number of surviving TH+ cells in the striatum compared with Nurr1-only cells (N) (**Fig. 8*G***). The average numbers of TH+ cells/animal at 8 wk of post-transplantation were NHB, 7339 ± 66; NM, 5758 ± 50 TH+ cell/animal; N, 1461 ± 18 TH+ cell/animal (n=5 animals/group; P<0.05 for NHB and NM *vs.* N). In addition to effects on cell survival, there were also marked differences in the degree of morphological maturation in grafted TH+ cells. NM- or NHB-derived TH+ cells within the graft exhibited mature neuronal morphologies with multiple long processes extending into the host striatum, while N-transduced TH+ cells were morphologically immature without any significant neurite arborization (Fig. 8*A–F*). The grafts were negative for the proliferation marker PCNA and free of any signs of tumor formation.

In vivo graft function was further assessed by measuring striatal DA levels. HPLC analysis revealed significantly increased levels of DA in NHB or NM grafts *vs.* N grafts: DA levels per tissue were NHB, 316.3 ± 28.6 μg/mg protein of graft; NM, 286.8 ± 32.5 μg/mg; N, 49.6 ± 14.7 μg/mg (n=3; P<0.05 for both NHB and NM *vs.* N).

Behavioral analysis was performed by measuring amphetamine-induced rotation behavior (Fig. 8*I*) and step-adjustment tests (Fig. 8*J*). Overall, animals grafted

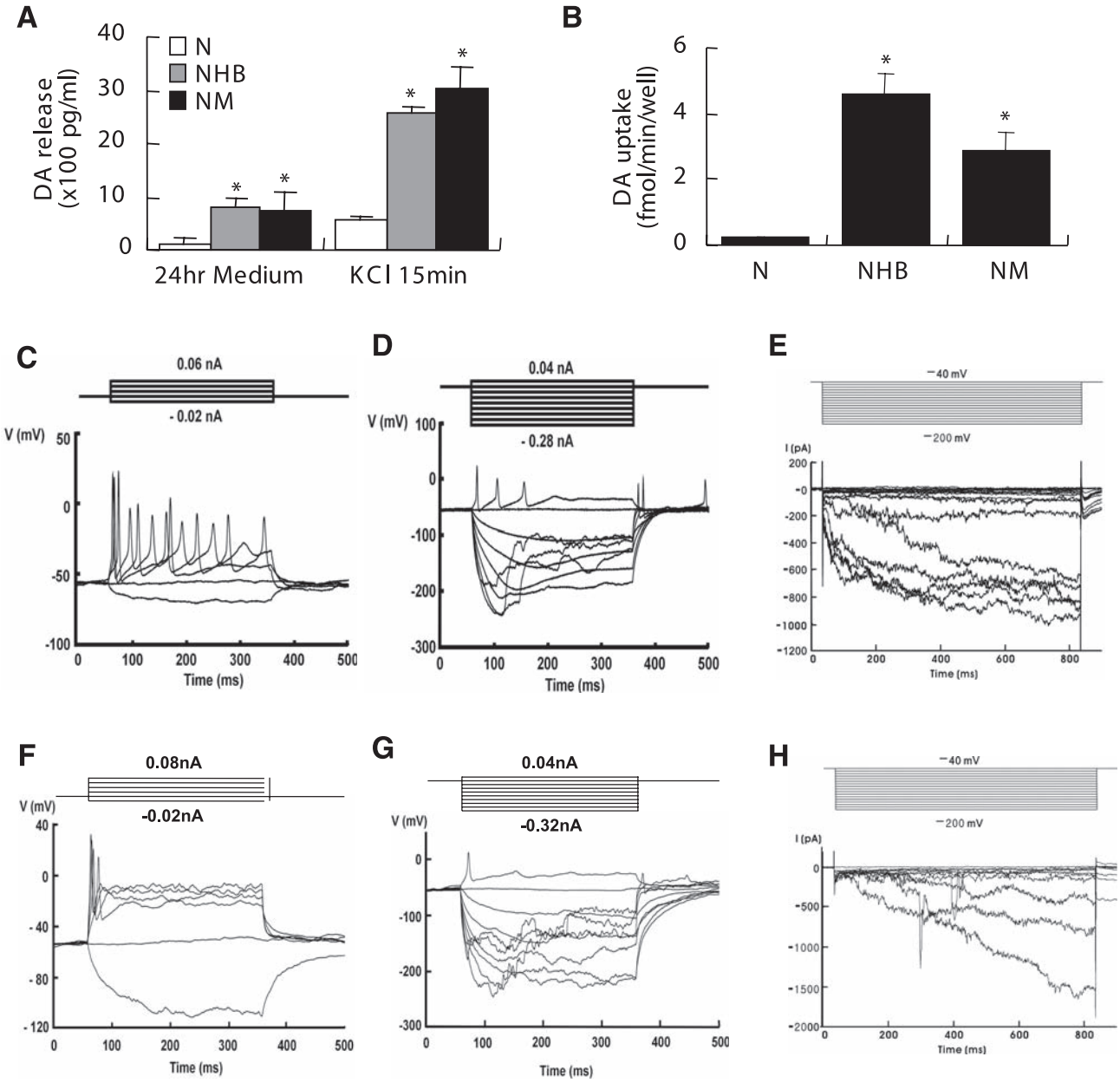

Figure 6. Biochemical and physiological analyses. Functional analyses were performed at day 10 of *in vitro* differentiation. *A)* HPLC determination of DA release. The graph shows DA levels in the medium conditioned for 24 h (24 h medium) and released by 56 mM KCl-evoked depolarization (KCl 15 min), $n = 3$. *B)* DAT-mediated specific DA uptake calculated by subtracting nonspecific uptake (with nomifensine) from total uptake, in N-, NM-, and NHB-transduced cultures ($n=5$ for each value). *Significantly different from the controls at $P < 0.01$. *C–H)* Electrophysiological properties of NHB- (*C–E*) and NM-transduced (*F–H*) cultures. Current-clamp recordings during injection of prolonged depolarizing currents elicited fast action potentials (*C*, *F*). *D*, *G*) Illustrate anomalous rectification in current-clamp recordings during prolonged injections of hyperpolarizing current, a feature highly characteristic of midbrain DA neurons. *E*, *H*) Traces show hyperpolarizing activated inward currents (Ih) in voltage clamping mode.

with NM- or NHB-tranduced cells demonstrated significant improvement in both parameters (Fig. 8*I*, *J* and supplementary Tables 1 and 2). Consistent with our published work (8), transplantation of precursors transduced with Nurr1 only (N) did not lead to significant behavioral restoration (Fig. 8*I*, *J*). These data suggest that expression of SHH and Bcl-XL or expression of Mash1 potentiates the *in vitro* and *in vivo* function of Nurr1-induced DA cells and that genetic manipulation of these genes may represent an important strategy for the development of donor cell sources suitable for cell therapy in PD.

DISCUSSION

In the present study, we identified several factors that modulate the morphological and functional differentiation of DA cells derived from Nurr1-expressed neural precursors. We demonstrated that morphological dif-

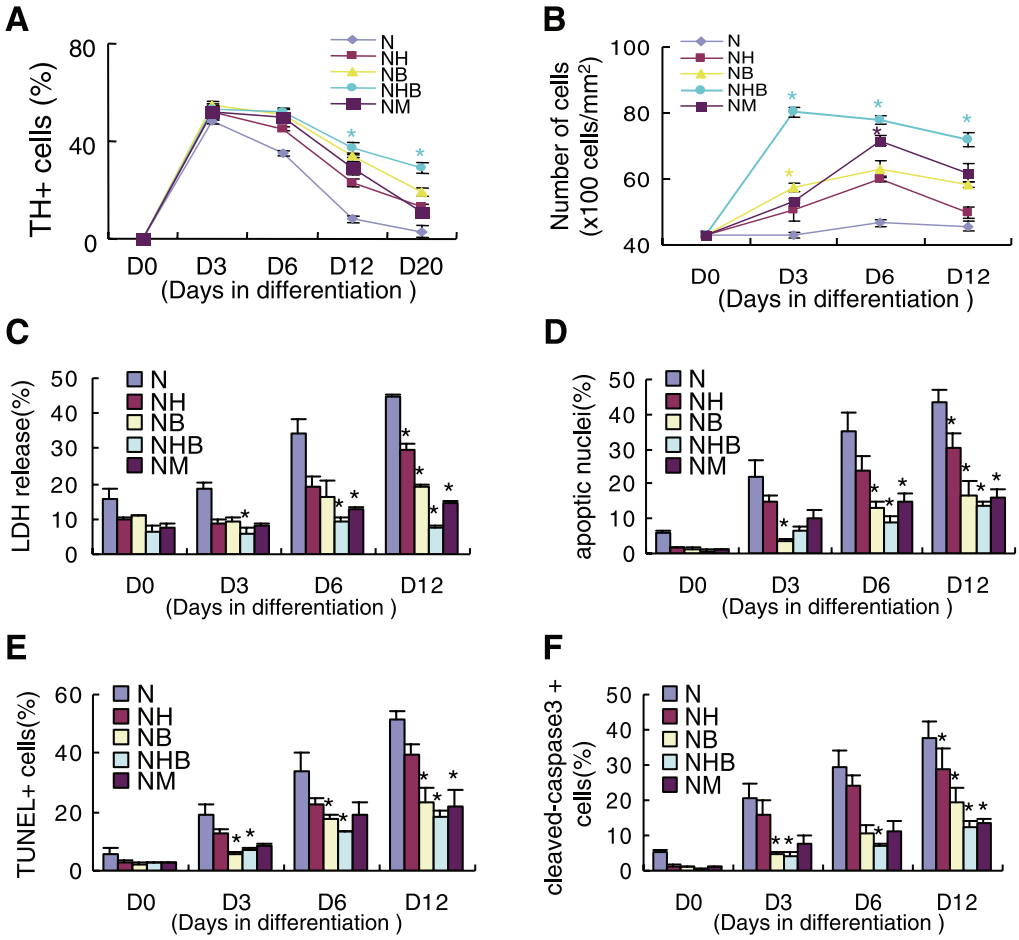

Figure 7. *In vitro* cell survival. *A)* %TH+ cells out of total DAPI+ cells. *B)* Number of total viable cells. *C)* % LDH release relative to total cellular LDH. *D)* % cells with fragmented and condensed apoptotic nuclei out of total DAPI+ cells. *E)* % TUNEL+ cells. *F)* % cleaved caspase 3+ cells. The passaged cultures of cortical precursor cells were prepared and transduced, as described. Cell viabilities were determined during cell differentiation day 0–12 or 20. Differentiation day 0 is the day when bFGF withdrawal was started. *Significantly different from the controls at $P < 0.05$.

ferentiation of Nurr1-DA cells is dependent on cell-to-cell contact and developmental stage of the cultured neural precursor cells. Our data further indicate that Bcl-XL and SHH are key factors controlling morphological maturation of Nurr1-DA cells and that expression of Bcl-XL and SHH transgenes was sufficient to drive the differentiation of Nurr1-tranduced precursor cells into mature DA neurons. Such precursor-derived DA neurons expressed key dopaminergic and neuronal markers and exhibited characteristic presynaptic DA neuron properties *in vitro*. Our findings are consistent with previous reports showing enhanced morphological differentiation and synaptic function in ES-derived and primary neurons by Bcl-XL (11, 36) and the promotion of neurite outgrowth through SHH-mediated chemoattraction (19, 43).

Our data demonstrate that expression of proneural bHLH transcription factors is an alternative approach for driving neuronal differentiation in Nurr1-induced DA cells *in vitro*. However, surprisingly, marked differences were found between the achaete-scute related bHLH factor Mash1 and the atonal-related bHLHs Ngn1 and Ngn2 in promoting DA neuron-specific differentiation. While Mash1 promoted the morphological and functional differentiation of Nurr1-induced DA cells, forced expression of Ngn1 or Ngn2 in Nurr1-transduced cells led to a repression of DA neuron phenotype. In agreement with these data, a recent study from our group (10) observed an inhibitory role of Ngns in Nurr1-induced transactivation of the TH promoter. We have also identified putative functional domains within the Mash1 and Ngn1 and 2 proteins responsible for the divergent role during Nurr1-DA differentiation. While these additional data provide a possible mechanistic link explaining the inhibitory role of Ngn1/Ngn2 on DA-specific differentiation in Nurr1-induced cells, two recent studies suggest an important positive role for Ngn2 in the development of mouse midbrain DA neurons *in vivo* (37, 38).

Numerous possibilities could explain the contrasting roles of Ngn2 between the *in vitro* data reported here and the data on midbrain developmental *in vivo*. First of all, differences in the timing of Ngn2 expression are clear. In our study, Ngn2 was expressed concomitantly to Nurr1 within the same cell, whereas Ngn2 is coexpressed in only a small population of Nurr1-expressing

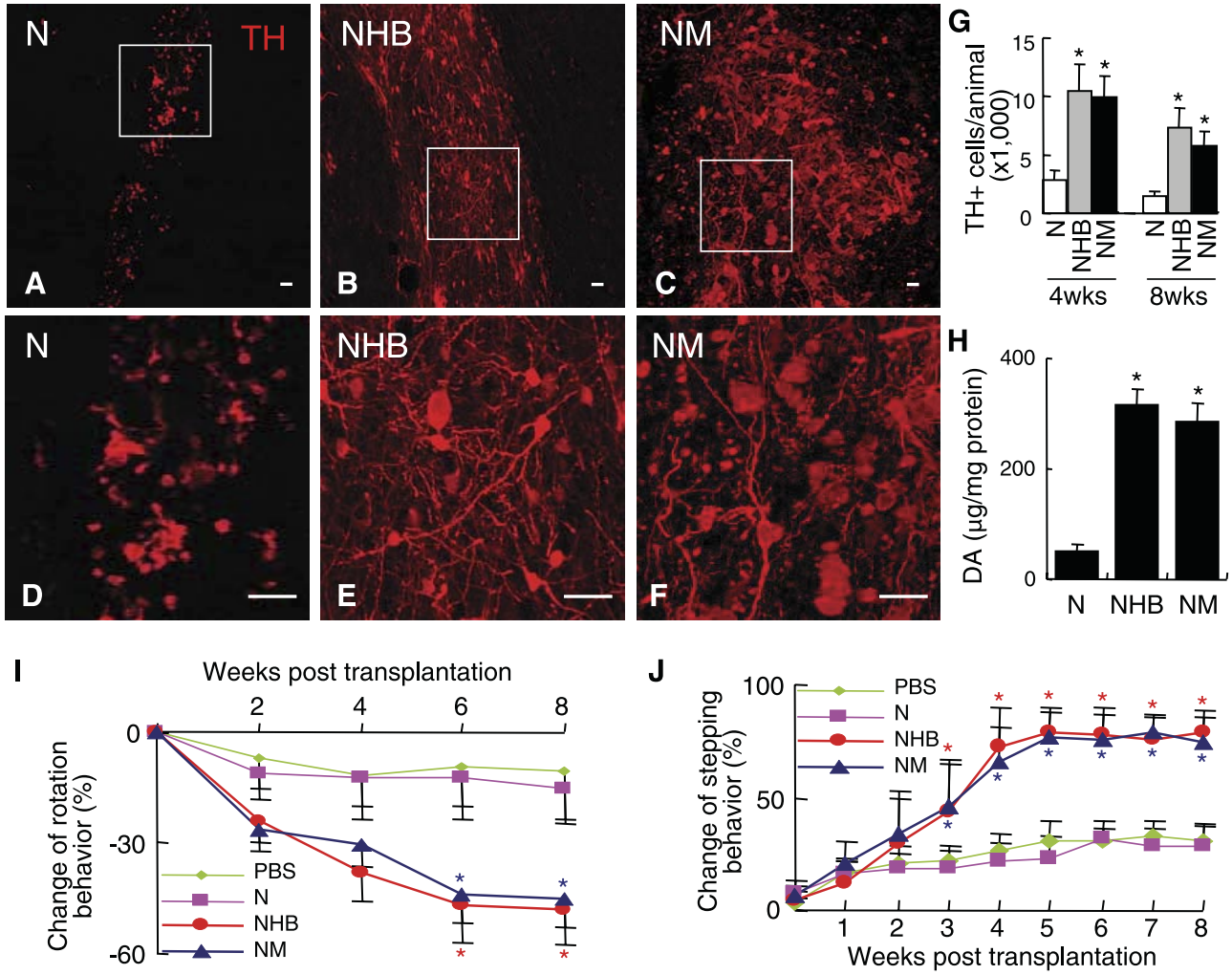

Figure 8. *In vivo* survival, differentiation and function of Nurr1-induced DA cells. *A–F)* Representative confocal images stacks (35 μm in z) of the TH+ striatal grafts at 4 wk after transplantation derived from precursors transduced with N (*A*, *D*), NHB (*B*, *E*) and NM (*C*, *F*). The boxed areas of (*A–C*) are magnified in (*D–F*). Scale bar, 20 μm. *G)* Quantification of TH+ cells in grafts at 4 and 8 wk after transplantation. *Significantly different from N-grafted at $P < 0.05$, $n = 5$ for each value. *H)* DA levels in grafts 8 wk after transplantation. *$P < 0.05$, $n = 5$ for each value. Behavioral recovery was assessed by amphetamine-induced rotation (*I*) and step adjustment tests (*J*) in shame-operated (PBS-injection, n=8), and animals grafted with precursors transduced with N (n=10), NHB (n=25), and NM (n=15). *Significantly different from shame-operated at $P < 0.05$.

cells during mouse midbrain development *in vivo*. In early midbrain development Ngn2 expression is restricted to the ventricular zone. Nurr1 expression is observed within the mantel zone of the ventral midbrain at slightly later developmental stages (37, 38). It is possible that Ngn2 has dual roles in the midbrain DA neuron development. While Ngn2 expression in early midbrain development prior to Nurr1 expression is required for the DA neuron formation, Ngn2 negatively regulates DA phenotype acquisition in the small population of the cells coexpressing Nurr1 at later developmental stages. Such the negative regulation of Ngn2 may serve to establish an appropriate number of DA cells in the developing midbrain. While such questions may be the basis for future studies aimed at more fully elucidating normal mechanisms of midbrain DA neuron development *in vivo*, our study was directed at defining the molecular steps to generate functional DA neurons from naive neuron precursor *in vitro*. In fact our data provide the first example of successfully manipulating naive nonmidbrain neural precursors toward a DA neuron phenotype that can restore behavioral deficits in a rodent model of PD.

Donor cell survival is a critical factor for the success of DA neuron transplantation in preclinical models of PD. Our study demonstrates enhanced *in vitro* and *in vivo* survival of Nurr1-induced DA cells transduced with SHH/Bcl-XL or with Mash1. The observed effects of Bcl-XL and SHH on the survival of Nurr1-induced DA cells can likely be explained by the well-established antiapoptotic roles of Bcl-XL and SHH in neuronal cells (34, 35). In contrast, Mash1-induced increase of DA cell survival was unexpected. Neuronal differentiation induced by neurogenic factors is often coupled with cell cycle arrest and apoptosis. We observed increased levels of SHH mRNAs in cultured precursor cells transduced with Mash1 but not in cultures transduced with Ngn1 or Ngn2 (Jo *et al.*, our unpublished

data). Thus, increased expression of SHH in Mash1-transduced cells may represent a possible mechanisms to explain survival effects on Nurr1-induced DA cells.

We finally demonstrated *in vivo* survival and functions of NHB- and NM-transduced precursor cells. Based on robust *in vivo* TH+ cell survival and DA production in NHB and NM grafts, it is reasonable to assume that the behavioral improvements are due to restored DA neurotransmission of graft-derived TH+ neurons. However, other groups have reported that some degree of behavioral recovery can be achieved through graft-derived trophic effects on the remaining endogenous DA population (39). SHH has previously shown efficacy as a pharmacological agent in preclinical models of PD (40–42). Thus, we cannot rule out that SHH secreted from NHB- and NM-transduced cells could have contributed to behavioral recovery.

In conclusion, our study demonstrates that the genetic manipulation of novel cofactors acting in concert with Nurr1 provide a powerful strategy to enhance the differentiation and function of precursor-derived DA neurons. Extensive functional characterization *in vitro* and *in vivo* suggests that DA neurons derived from naive neural precursors adopt properties characteristic of midbrain type DA neurons. Finally, our study provides the first example for achieving functional restoration in Parkinsonian rats using DA neurons derived from naive nonmidbrain-derived neural precursors. The use of genetically manipulated forebrain precursors could provide an interesting alternative to the use of human fetal midbrain tissue given the availability and scalability of human forebrain progenitors. However, it remains to be determined whether our approach is applicable to human cells, and whether the risk of introducing multiple transgenes is manageable in a therapeutic setting. FJ

We thank Dr. Arnon Rosenthal for Smo-M2 cDNA and Dr. Haeyoung Suh-Kim for N-SHH cDNA. This work was supported by SC2130 and SC2150 (Stem Cell Research Center of the 21st Century Frontier Research Program) funded by the Ministry of Science and Technology, Republic of Korea.

REFERENCES

1. McKay, R. D. (1997) Stem cells in the central nervous system. *Science* **276,** 66–71
2. Piccini, P., Brooks, D. J., Bjorklund, A., Gunn, R. N., Grasby, P. M., Rimoldi, O., Brundin, P., Hagell, P., Rehncrona, S., Widner, H., and Lindvall, O. (1999) Dopamine release from nigral transplants visualized *in vivo* in a Parkinson's patient. *Nat. Neurosci.* **2,** 1137–1140
3. Lee, J. Y., Koh, H. C., Chang, M. Y., Park, C. H., Lee, Y. S., and Lee, S. H. (2003) Erythropoietin and bone morphogenetic protein 7 mediate ascorbate-induced dopaminergic differentiation from embryonic mesencephalic precursors. *Neuroreport* **14,** 1401–1404
4. Yan, J., Studer, L., and McKay, R. D. (2001) Ascorbic acid increases the yield of dopaminergic neurons derived from basic fibroblast growth factor expanded mesencephalic precursors. *J. Neurochem.* **76,** 307–311
5. Zetterstrom, R. H., Solomin, L., Jansson, L., Hoffer, B. J., Olson, L., and Perlmann, T. (1997) Dopamine neuron agenesis in Nurr1-deficient mice. *Science* **276,** 248–250
6. Saucedo-Cardenas, O., Quintana-Hau, J. D., Le, W. D., Smidt, M. P., Cox, J. J., De Mayo, F., Burbach, J. P., and Conneely, O. M. (1998) Nurr1 is essential for the induction of the dopaminergic phenotype and the survival of ventral mesencephalic late dopaminergic precursor neurons. *Proc. Natl. Acad. Sci. U. S. A.* **95,** 4013–4018
7. Castillo, S. O., Baffi, J. S., Palkovits, M., Goldstein, D. S., Kopin, I. J., Witta, J., Magnuson, M. A., and Nikodem, V. M. (1998) Dopamine biosynthesis is selectively abolished in substantia nigra/ventral tegmental area but not in hypothalamic neurons in mice with targeted disruption of the Nurr1 gene. *Mol. Cell. Neurosci.* **11,** 36–46
8. Kim, J. Y., Koh, H. C., Lee, J. Y., Chang, M. Y., Kim, Y. C., Chung, H. Y., Son, H., Lee, Y. S., Studer, L., McKay, R., and Lee, S. H. (2003) Dopaminergic neuronal differentiation from rat embryonic neural precursors by Nurr1 overexpression. *J. Neurochem.* **85,** 1443–1454
9. Johe, K. K., Hazel, T. G., Muller, T., Dugich-Djordjevic, M. M., and McKay, R. D. (1996) Single factors direct the differentiation of stem cells from the fetal and adult central nervous system. *Genes Dev.* **15,** 3129–3140
10. Park, C. H., Kang, J. S., Kim, J. S., Chung, S., Koh, J. Y., Yoon, E. H., Jo, A. Y., Chang, M. Y., Koh, H. C., Hwang, S., Suh-Kim, H., Lee, Y. S., Kim, K. S., and Lee, S. H. (2006) Differential actions of the proneural genes Mash1 and Neurogenins in Nurr1-induced dopamine neuron differentiation. *J. Cell Sci.* **119,** 2310–2320
11. Shim, J. W., Koh, H. C., Chang, M. Y., Roh, E., Choi, C. Y., Oh, Y. J., Son, H., Lee, Y. S., Studer, L., and Lee, S. H. (2004) Enhanced *in vitro* midbrain dopamine neuron differentiation, dopaminergic function, neurite outgrowth, and 1-methyl-4-phenylpyridium resistance in mouse embryonic stem cells overexpressing Bcl-XL. *J. Neurosci.* **24,** 843–852
12. Park, C. H., Minn, Y. K., Lee, J. Y., Choi, D. H., Chang, M. Y., Shim, J. W., Ko, J. Y., Koh, H. C., Kang, M. J., Kang, J. S., Rhie, D. J., Lee, Y. S., Son, H., Moon, S. Y., Kim, K. S., and Lee, S. H. (2005) In vitro and *in vivo* analyses of human embryonic stem cell-derived dopamine neurons. *J. Neurochem.* **92,** 1265–1276
13. Olsson, M., Nikkhah, G., Bentlage, C., and Bjorklund, A. (1995) Forelimb akinesia in the rat Parkinson model: differential effects of dopamine agonists and nigral transplants as assessed by a new stepping test. *J. Neurosci.* **15,** 3863–3875
14. Sakurada, K., Ohshima-Sakurada, M., Palmer, T. D., and Gage, F. H. (1999) Nurr1, an orphan nuclear receptor, is a transcriptional activator of endogenous tyrosine hydroxylase in neural progenitor cells derived from the adult brain. *Development* **126,** 4017–4026
15. Wagner, J., Akerud, P., Castro, D. S., Holm, P. C., Canals, J. M., Snyder, E. Y., Perlmann, T., and Arenas, E. (1999) Induction of a midbrain dopaminergic phenotype in Nurr1-overexpressing neural stem cells by type 1 astrocytes. *Nat. Biotechnol.* **17,** 653–659
16. Chang, M. Y., Park, C. H., Lee, S. Y., and Lee, S. H. (2004) Properties of cortical precursor cells cultured long term are similar to those of precursors at later developmental stages. *Dev. Br. Res.* **153,** 89–96
17. Hynes, M., Porter, J. A., Chiang, C., Chang, D., Tessier-Lavigne, M., Beachy, P. A., and Rosenthal, A. (1995) Induction of midbrain dopaminergic neurons by Sonic hedgehog. *Neuron* **15,** 35–44
18. Ye, W., Shimamura, K., Rubenstein, J. L., Hynes, M. A., Rosenthal, A. (1998) FGF and Shh signals control dopaminergic and serotonergic cell fate in the anterior neural plate. *Cell* **29,** 755–766
19. Charron, F., Stein, E., Jeong, J., McMahon, A. P., and Tessier-Lavigne, M. (2003) The morphogen sonic hedgehog is an axonal chemoattractant that collaborates with netrin-1 in midline axon guidance. *Cell* **4,** 11–23
20. Hynes, M., Ye, W., Wang, K., Stone, D., Murone, M., Sauvage, F., and Rosenthal, A. (2000) The seven-transmembrane receptor smoothened cell-autonomously induces multiple ventral cell types. *Nat. Neurosci.* **3,** 41–46
21. Chen, J. K., Taipale, J., Cooper, M. K., and Beachy, P. A. (2002) Inhibition of Hedgehog signaling by direct binding of cyclopamine to Smoothened. *Genes Dev.* **16,** 2743–2748
22. Chang, M. Y., Son, H., Lee, Y. S., and Lee, S. H. (2003) Neurons and astrocytes secretes factors that cause stem cells to differen-

tiate into neurons and astrocytes, respectively. *Mol. Cell. Neurosci.* **23,** 414–426
23. Quinn, S. M., Walters, W. M., Vescovi, A. L., and Whittemore, S. R. (1999) Lineage restriction of neuroepithelial precursor cells from fetal human spinal cord. *J. Neurosci. Res.* **57,** 590–602
24. Holm, K. H., Cicchetti, F., Bjorklund, L., Boonman, Z., Tandon, P., Costantini, L. C., Deacon, T. W., Huang, X., Chen, D. F., and Isacson, O. (2001) Enhanced axonal growth from fetal human bcl-2 transgenic mouse dopamine neurons transplanted to the adult rat striatum. *Neuroscience* **104,** 397–405
25. Oh, Y. J., Swarzenski, B. C., O'Malley, K. L. (1996) Overexpression of Bcl-2 in a murine dopaminergic neuronal cell line leads to neurite outgrowth. *Neurosci. Lett.* **202,** 161–164
26. Kageyama, R., and Nakanishi, S. (1997) Helix-loop-helix factors in growth and differentiation of the vertebrate nervous system. *Curr. Opin. Genet. Dev.* **7,** 659–665
27. Lee, J. E. (1997) Basic helix-loop-helix genes in neural development. *Curr. Opin. Neurobiol.* **7,** 13–20
28. Bertrand, N., Castro, D. S., and Guillemot, F. (2002) Proneural genes and the specification of neural cell types. *Nat. Rev. Neurosci.* **3,** 517–530
29. Ross, S. E., Greenberg, M. E., and Stiles, C. D. (2003) Basic helix-loop-helix factors in cortical development. *Neuron* **39,** 13–25
30. Modolell, J. (1997) Patterning of the adult peripheral nervous system of Drosophila. *Perspect. Dev. Neurobiol.* **4,** 285–296
31. Campos-Ortega, J. A. (1998) The genetics of the Drosophila achaete-scute gene complex: a historical appraisal. *Int. J. Dev. Biol.* **42,** 291–297
32. Rayport, S., Sulzer, D., Shi, W. X., Sawasdikosol, S., Monaco, J., Batson, D., and Rajendran, G. (1992) Identified postnatal mesolimbic dopamine neurons in culture: morphology and electrophysiology. *J. Neurosci.* **12,** 4264–4280
33. Rohrbacher, J., Ichinohe, N., and Kitai, S. T. (2000) Electrophysiological characteristics of substantia nigra neurons in organotypic cultures: spontaneous and evoked activities. *Neuroscience* **97,** 703–714
34. Thibert, C., Teillet, M. A., Lapointe, F., Mazelin, L., Le Douarin, N. M., and Mehlen, P. (2003) Inhibition of neuroepithelial patched-induced apoptosis by sonic hedgehog. *Science* **301,** 843–846
35. Miao, N., Wang, M., Ott, J. A., D'Alessandro, J. S., Woolf, T. M., Bumcrot, D. A., Mahanthappa, N. K., and Pang, K. (1997) Sonic hedgehog promotes the survival of specific CNS neuron populations and protects these cells from toxic insult i*n vitro*. *J. Neurosci.* **1,** 5891–5899
36. Jonas, E. A., Hoit, D., Hickman, J. A., Brandt, T. A., Polster, B. M., Fannjiang, Y., McCarthy, E., Montanez, M. K., Hardwick, J. M., and Kaczmarek, L. K. (2003) Modulation of synaptic transmission by the BCL-2 family protein Bcl-XL. *J. Neurosci.* **23,** 8423–8431
37. Kele, J., Simplicio, N., Ferri, A. L., Mira, H., Guillemot, F., Arenas, E., and Ang, S. L. (2006) Neurogenin 2 is required for the development of ventral midbrain dopaminergic neurons. *Development* **133,** 495–505
38. Andersson, E., Jensen, J. B., Parmar, M., Guillemot, F., and Bjorklund, A. (2006) Development of the mesencephalic dopaminergic neuron system is compromised in the absence of neurogenin 2. *Development* **133,** 507–16
39. Ourednik, J., Ourednik, V., Lynch, W. P., Schachner, M., and Snyder, E. Y. (2002) Neural stem cells display an inherent mechanism for rescuing dysfunctional neurons. *Nat. Biotechnol.* **20,** 1103–1110
40. Tsuboi, K., and Shults, C. W. (2002) Intrastriatal injection of sonic hedgehog reduces behavioral impairment in a rat model of Parkinson's disease. *Exp. Neurol.* **173,** 95–104
41. Dass, B., Iravani, M. M., Huang, C., Barsoum, J., Engber, T. M., Galdes, A., and Jenner, P. (2005) Sonic hedgehog delivered by an adeno-associated virus protects dopaminergic neurones against 6-OHDA toxicity in the rat. *J. Neural. Transm.* **112,** 763–778
42. Rafuse, V. F., Soundararajan, P., Leopold, C., and Robertson, H. A. (2005) Neuroprotective properties of cultured neural progenitor cells are associated with the production of sonic hedgehog. *Neuroscience* **131,** 899–916
43. So, P.-L., Yip, P. K., Bunting, S., Wong, L.-F., Mazarakis, N. D., Hall, S., McMahon, S., Maden, M., and Corcoran, J. P. T. (2006) Interactions between retinoic acid, nerve growth factor and sonic hedgehog signalling pathways in neurite outgrowth. *Dev. Biol.* **298,** 167–175

Received for publication March 28, 2006.
Accepted for publication July 11, 2006.

Acquisition of *in vitro* and *in vivo* functionality of Nurr1-induced dopamine neurons

Chang-Hwan Park,[*,§] Jin Sun Kang,[*,§] Yeon Ho Shin,[*,§] Mi-Yoon Chang,[†,§] Seungsoo Chung,[‖] Hyun-Chul Koh,[‡,§] Mei Hong Zhu,[¶] Seog Bae Oh,[¶] Yong-Sung Lee,[†,§] Georgia Panagiotakos,[**] Vivian Tabar,[**] Lorenz Studer,[**] and Sang-Hun Lee[†,§,1]

Departments of *Microbiology, [†]Biochemistry and Molecular Biology, and [‡]Pharmacology, College of Medicine, and [§]Institute of Mental Health, Hanyang University, Seoul, Korea; [‖]Department of Physiology, College of Medicine, Yonsei University, Seoul, Korea; [¶]Department of Physiology, College of Dentistry and Dental Research Institute, Seoul National University, Seoul, Korea; and **Laboratory of Stem Cell and Tumor Biology, Neurosurgery and Developmental Biology, Sloan Kettering Cancer Institute, New York, New York, USA

To read the full text of this article, go to http://www.fasebj.org/cgi/doi/10.1096/fj.06-6159fje

SPECIFIC AIMS

The derivation of functional dopamine (DA) neurons from proliferating neural precursor or stem cell populations has been an important goal in the development of cell-based therapies for the treatment of Parkinson's Disease (PD). The primary goal of the present study was the identification of a set of genetic factors sufficient for directing the differentiation of naive neural precursors into fully functional DA neurons that can reverse behavioral deficits in Parkinsonian rats.

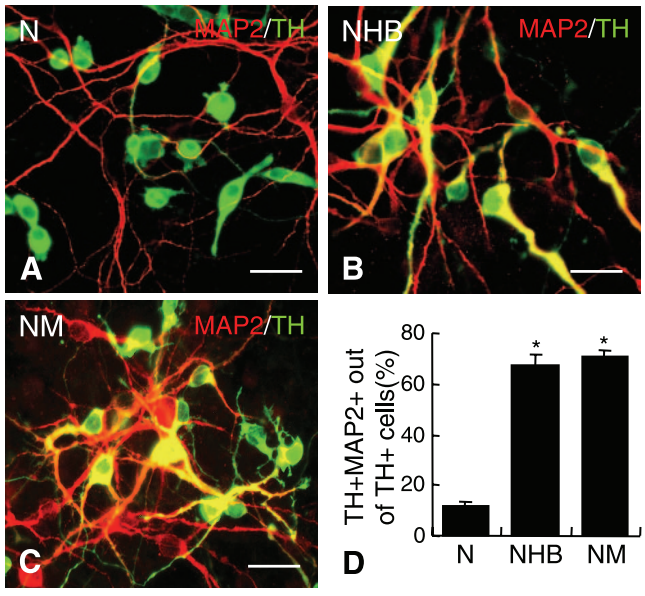

Figure 1. Expression of the mature neuron marker MAP2 in Nurr1-induced TH cells. Immunocytochemistry was carried out at day 10 of *in vitro* differentiation in the cultures transduced with Nurr1 alone (N), Nurr1+SHH+Bcl-XL (NHB), and Nurr1+Mash1 (NM). Note that TH+ cells in NHB and NM-cultures exhibit mature neuronal morphologies with multiple processes. Graph D represents the percentages of TH+ cells coexpressing MAP2 out of total TH+ cells *Significantly different from N control with the *P* value of <0.001. Scale bar, 10 μm.

PRINCIPAL FINDINGS

1. Sonic hedgehog (SHH), Bcl-XL, and Mash1 induce morphological differentiation in Nurr1-induced DA cells

Neural precursor cells were isolated from the developing rat cortex, and proliferated *in vitro* by basic fibroblast growth factor (bFGF). Cultured cortical precursors were retrovirally tranduced with Nurr1, an orphan nuclear receptor specific to midbrain DA neuron development. Cells were differentiated for several days prior to analysis. As reported previously, ectopic expression of Nurr1 efficiently induced the expression of the DA neuron marker tyrosine hydroxylase (TH) but resulted in poor morphological and functional differentiation of the cells (**Fig. 1*A***). We tried to define additional genetic factors for the neuronal differentiation and functional acquisition of Nurr1-induced DA cells.

We initiated this study by comparing morphologic differentiation of Nurr1-DA cells in various cultures such as passaged (P1) *vs.* unpassaged (P) cultures, and cultures derived from different developmental stages. Our comparative analyses of the different culture conditions suggested SHH and Bcl-XL as candidate genes for the morphologic differentiation of Nurr1-DA cells. Co-expression of SHH along with Nurr1 (Bicistronic Nurr1-IRES-SHH, NH) extensively increased TH fiber length in Nurr1-induced DA cells, compared with cell

[1] Correspondence: Department of Biochemistry and Molecular Biology, College of Medicine, Hanyang University, #17 Haengdang-dong, Sungdong-gu, Seoul, 133–791 Korea. E-mail: leesh@hanyang.ac.kr

doi: 10.1096/fj.06-6159fje

transduced with Nurr1 alone (N). Previous studies have demonstrated Bcl-XL-mediated morphologic maturation and synaptic function of neuronal cells. Expectedly, cells transduced with Nurr1-IRES-Bcl-XL (NB) exhibited a marked increase in TH fibers of Nurr1-DA cells. Additional studies showed that SHH and Bcl-XL have additive effects in the morphologic differentiation (TH fiber length per Nurr1-DA cell were Nurr1-IRES-SHH-IRES-Bcl-XL (NHB): 82.5 ± 1.5 μm, NH: 38.0 ± 5.8 μm, NB: 62.2 ± 6.1 μm, N: 10.3 ± 0.6 μm, Fig. 1*B, D*).

Neuronal basic-helix-loop-helix (bHLH) transcriptional factors are known to play an essential role in the neuronal specification of precursor cells and to promote the morphological and functional maturation of postmitotic neurons. Forced expression of the bHLH factor Mash1 (Nurr1-IRES-Mash1 retrovirus (NM)), caused a dramatic increase in TH+ fiber length of the Nurr1-DA cells (NM: 147.4±50.9 μm *vs.* N: 9.0±1.8 μm, Fig. 1*C, D*).

2. Analysis of *in vitro* presynaptic neuronal function in Nurr1-induced DA cells

We next examined whether enhanced morphological maturation is correlated with the expression of mature neuronal and dopaminergic markers and the acquisition of presynaptic DA neuron function. Coexpression of SHH+Bcl-XL (NHB) or Mash1 (NM) greatly enhanced the percentage of Nurr1-induced DA cells expressing MAP2, a mature neuronal marker. The percentages of all TH+ cells expressing MAP2 were NHB: 67.5 ± 4.1%; NM: 71.0 ± 2.4%; N: 11.8 ± 2.1% (Fig. 1). Measurements of DA release by HPLC showed significant differences among the various group of Nurr1 induced DA cells. Levels of DA on depolarization (56 mM KCl) were NHB: 2558.2 ± 152.4 pg/ml; NM: 3049.9 ± 377.6 pg/ml; and N: 561.2 ± 50.2 pg/ml. Functional differences in DA metabolism were further illustrated by measuring dopamine transporter (DAT)-mediated high-affinity reuptake

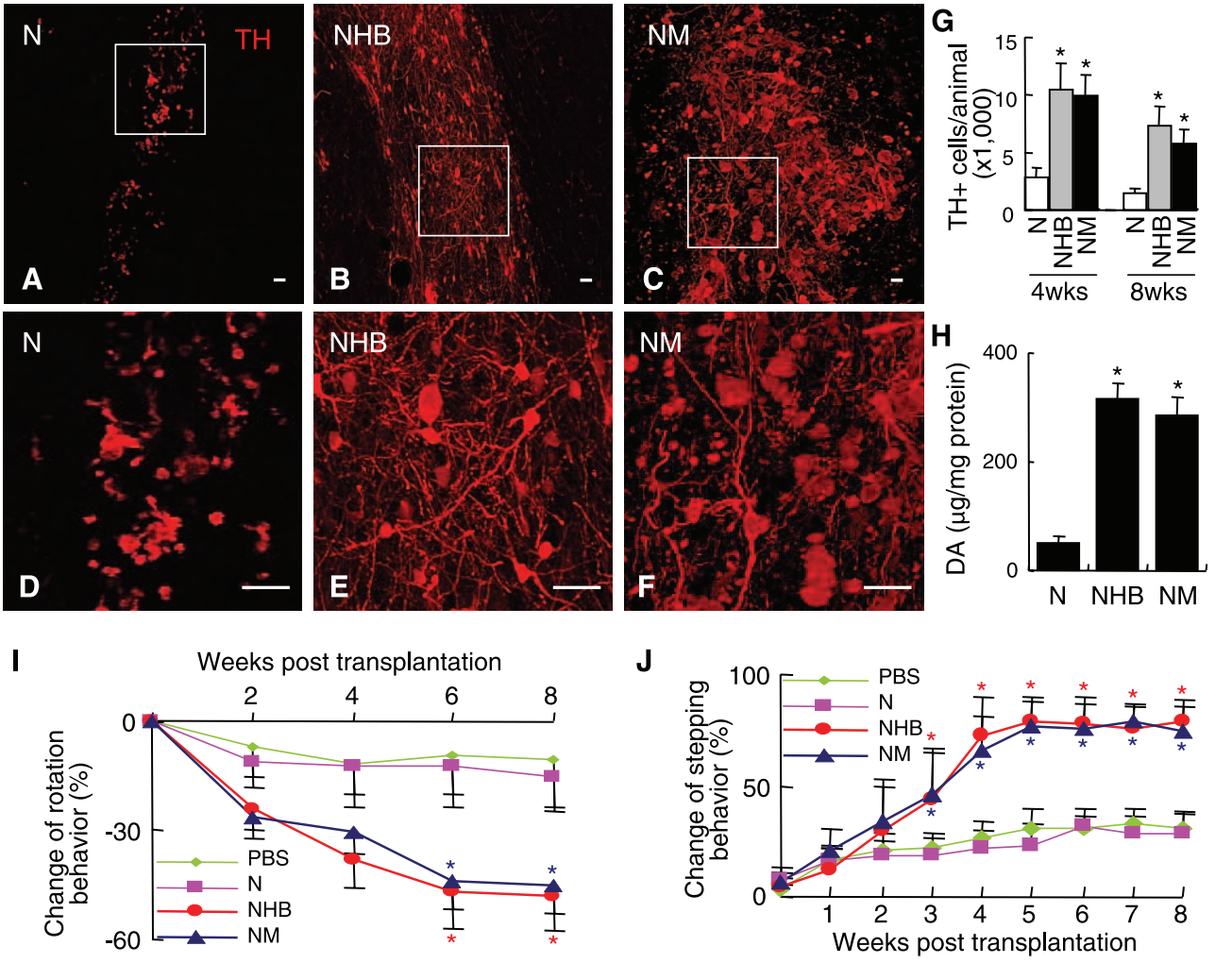

Figure 2. *In vivo* survival, differentiation and function of Nurr1-induced DA cells. *A–F)* Representative confocal images stacks (35 μm in z) of the TH+ striatal grafts at 4 wk after transplantation derived from precursors transduced with N (*A, D*), NHB (*B, E*) and NM (*C, F*). The boxed areas of (*A–C*) are magnified in (*D–F*). Scale bar, 20 μm. *G)* Quantification of TH+ cells in grafts at 4 and 8 wk after transplantation. *Significantly different from N-grafted at $P < 0.05$, $n = 5$ for each value. *H)* DA levels in grafts 8 wk after transplantation. *$P < 0.05$, $n = 5$ for each value. Behavioral recovery was assessed by amphetamine-induced rotation (I) and step adjustment tests (J) in shame-operated (PBS-injection, n=8), or animals grafted with precursors transduced with N (n=10), NHB (n=25), and NM (n=15). *Significantly different from shame-operated at $P < 0.05$.

of DA. While levels of reuptake in Nurr1 cultures were at the limit of detection (N: 0.23±0.01 fmol/min/well), NHB- and NM-transduced cells exhibited robust DA uptake (NHB: 4.59±0.50 fmol/min/well; NM: 2.90±0.61 fmol/min/well). Electrophysiological analyses of Nurr1-induced DA cells in NHB- and NM-transduced cultures demonstrated well-developed sodium and potassium channels, and the generation of action potentials on injection of depolarizing currents. In addition to general neuronal features, electrophysiological analyses also revealed properties characteristic for mesolimbic and nigrostriatal DA neurons. DA characteristic features included anomalous rectification, the time-dependent reduction in the membrane deflection, which was observed on injection of hyperpolarizing currents at increasing intensities.

3. *In vivo* transplantation studies

The final set of experiments was directed at addressing the capacity of transplanted Nurr1-induced DA cells for *in vivo* survival, integration, and function in Parkinsonian rats.

At 4 and 8 wk after intrastriatal transplantation, grafts derived from NHB- and NM-transduced precursors showed a dramatic increase in the number of surviving TH+ cells compared with grafts of Nurr1-only (N) transduced cells (**Fig. 2*A–C*** and ***G***). In addition to effects on cell survival, there were also marked differences in the degree of morphological maturation in grafted TH+ cells. NM- or NHB-derived TH+ cells within the graft exhibited mature neuronal morphologies with multiple long processes extending into the host striatum, while Nurr1-transduced TH+ cells (N) were morphologically immature without significant neurite extension (Fig. 2*A–F*).

In vivo graft function was assessed by measuring striatal DA levels. HPLC analysis revealed significantly increased levels of DA in NHB or NM grafts *vs.* N grafts: DA levels in the grafted tissues were NHB, 316.3 ± 28.6 μg/mg protein of graft; NM, 286.8 ± 32.5 μg/mg; N, 49.6 ± 14.7 μg/mg (n=3; P<0.05 for both NHB and NM *vs.* N; Fig. 2*H*).

Behavioral analysis was performed by measuring amphetamine-induced rotation behavior (Fig. 2*I*) and step adjustment tests (Fig. 2*J*). Animals grafted with NHB or NM-tranduced cells demonstrated significant improvement in both parameters. Consistent with our published work, transplantation of precursors transduced with Nurr1 only (N) did not lead to significant behavioral restoration. These data suggest that expression of SHH and Bcl-XL or expression of Mash1 potentiates the *in vitro* and *in vivo* function of Nurr1-induced DA cells and that genetic manipulation of these genes serves as a powerful strategy toward the development of donor cell sources suitable for cell replacement in PD.

CONCLUSIONS AND SIGNIFICANCE

Our study demonstrates that combinatorial genetic manipulations acting in concert with Nurr1 provide an efficient strategy to generate functional DA neurons from non-dopaminergic neural precursors (**Fig. 3**). Extensive functional characterizations *in vitro* and *in vivo* suggest these DA neurons generated *in vitro* from dividing forebrain precursors adopt biochemical and physiological properties characteristic of midbrain type DA neurons. Finally, our study provides the first example for achieving functional restoration in Parkinsonian rats using DA neurons derived from naive nonmidbrain-derived neural precursors. The use of genetically manipulated forebrain precursors could provide an interesting alternative to the use of human fetal midbrain tissue given the availability and scalability of human forebrain progenitors. However, it remains to be determined whether our approach is applicable to human cells and whether the risk of introducing multiple transgenes is manageable in a therapeutic setting.

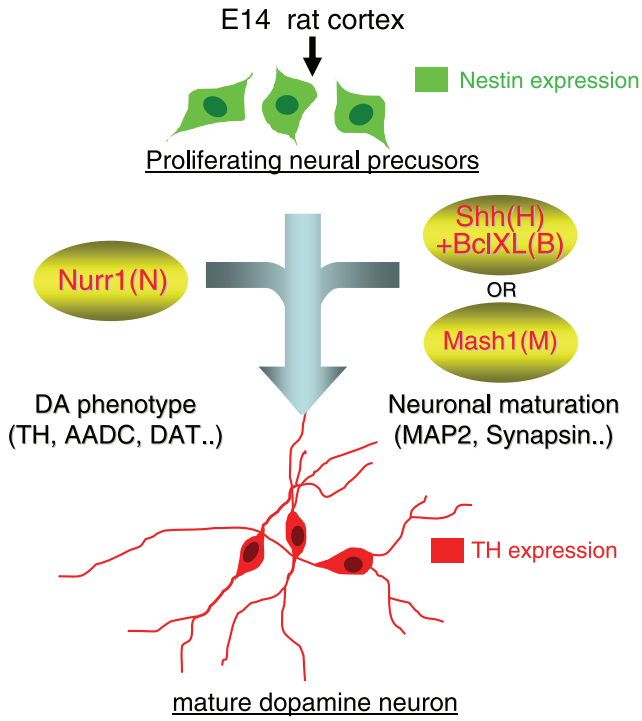

	-	N	NHB	NM
DA phenotype	-	++	++	++
Morphologic maturation	ND*	+/-	++	+++
In vitro presynaptic function	ND*	+/-	++	++
In vivo function in PD rat	ND*	-	++	++

* ND, not defined

Figure 3. Schematic drawing for the *in vitro* generation of functional DA neurons from cultured neural precursor cells. Transgene expression of Nurr1 (N) sufficiently induces DA phenotype expression in embryonic cortical precursor cells. Coexpression of SHH (H)+Bcl-XL (B) or Mash1 (M) drives Nurr1-expressing precursors to differentiate into morphologically and functionally mature DA neurons. The combinatorial genetic manipulation of Nurr1-SHH-Bcl-XL (NHB) or Nurr1-Mash1 (NM), therefore, provides an efficient strategy to generate midbrain DA neurons exhibiting *in vitro* and *in vivo* functions in PD rats.